Communication Strategies for Colonization Mission to Mars

A Thesis Submitted to the Faculty of
Universidad Carlos III de Madrid

In Partial Fulfillment of the
Requirements for the
Bachelor's Degree in Aerospace Engineering

By
Pablo A. Machuca Varela

June 2015

Dedicated to my dear mother, Teresa, for her education and inspiration; for making me the person I am today. And to my grandparents, Teresa and Hernán, for their care and love; for being the strongest motivation to pursue my goals.

Acknowledgments

I would like to thank my advisor, Professor Manuel Sanjurjo-Rivo, for his help and guidance along the past three years, and for his advice on this thesis. Professor Sanjurjo-Rivo first accepted me as his student and helped me discover my passion for the Orbital Mechanics research area. I am very thankful for the opportunity Professor Sanjurjo-Rivo gave me to do research for the first time, which greatly helped me improve my knowledge and skills as an engineer. His valuable advice also encouraged me to take Professor Howell's Orbital Mechanics course and Professor Longuski's Senior Design course while at Purdue University, as an exchange student, which undoubtedly enhanced my desire, and created the opportunity, to become a graduate student at Purdue University.

I would like to thank Sarag Saikia, the Mission Design Advisor of Project Aldrin-Purdue, for his exemplary passion and enthusiasm for the field. Sarag is responsible for making me realize the interest and relevance of a Mars communication network. He encouraged me to work on this thesis, and advised me along the way. I highly appreciate his advice and guidance to achieve my academic goals as well, and for making me dream of a brighter future.

I would like to give special thanks to Emily Zimovan, the Mission Design Team Leader of Project Aldrin-Purdue, for her collaboration and contribution to this project. Emily helped me analyze the S1L1 cycler trajectory in the circular-coplanar model, had the original idea of using the cycler vehicles as communication relays, and found the orbit opportunities for the cyclers in STOUR. She performed an exceptional work as a team leader and I greatly enjoyed the innumerous hours we worked together. I am very grateful to have met Emily, and to have had her as a classmate and as a teammate; and most importantly, I am very grateful to have Emily as a friend.

I must thank Universidad Carlos III de Madrid and Purdue University for the opportunity to study abroad in the US, which consequently opened up the door to a whole new spectrum of personal, academic and professional experiences and possibilities.

I would like to express my deepest gratitude to Madison Neuenschwander, for her support, motivation and love over the past year. She encouraged me to follow my dreams, she made me recognize my deepest passions and motivations, challenged my perspective and beliefs, and helped me change and grow as a person. I feel extremely fortunate to have Madison in my life.

I would like to thank my family in Chile: cousins (Cristian, Rolo, Dani and Paula), aunts (Marcela and Cristina), uncles (Andoni and Rolando–may he rest in peace) and grandparents (Teresa and Hernán), for being the reason I pursue my goals; for their care and love that remained strong despite the distance.

Last, I would like to thank my mother, Teresa, for her brave effort and sacrifice to provide a life full of ready-to-be-opened doors to her children: my brother (Sebastián) and myself. She has become my biggest inspiration, and she taught me the values and principles that make me the person I am today. I would like to dedicate this thesis, in particular, to her, together with all I have ever achieved; as everything I have ever done, and everything I will ever do, is thanks to the opportunities she helped me realize I now have.

Abstract

Earth-Mars cycler trajectories could be used as a periodic and cost-efficient human transportation system from Earth to Mars in a future mission to colonize Mars. Continuous and reliable communication between Mars and the Earth will be required in such a mission. In a circular-coplanar model, the existance of a particularly interesting cycler trajectory (ballistic outbound Earth-Mars S1L1 cycler trajectory) is proven, which has relatively short Earth-Mars transfer times, low relative velocities with respect to the planets at the encounters, and an intermediate Earth encounter within every two-synodic-period cycle. Two outbound Earth-Mars S1L1 cycler vehicles launched one synodic period apart could be used to maximize the number of trips from Earth to Mars. A new and economic method to maintain communication over periods of direct Earth-Mars link blockage (i.e. Earth-Mars solar conjunction) is introduced for a mission such that two outbound Earth-Mars S1L1 cycler vehicles are used for human transportation to Mars, using the cycler vehicles also as communication relays to avoid the need of a heliocentric communications satellite constellation to communicate from and to Mars. The analysis is performed in a circular-coplanar model and in a more realistic model (i.e. ephemeris model for the states of Earth and Mars, and STOUR results for the orbit parameters of the cycler trajectories). Continuous communication with only one cycler vehicle in orbit is proven not to be possible. In a mission with permanent human settlements on Mars and Phobos (inside Stickney Crater), two two-satellite Mars-centered communication constellations are designed (in a circular-coplanar model) to continuously communicate the colonies on Phobos and Mars, and the Earth (directly or through the cycler vehicles), which could avoid the need of a three- or four-satellite constellation around Mars. A communication constellation consisted of two satellites in a stationary orbit around Mars is determined to be a more cost-efficient solution than two satellites in Phobos' orbit. The link performance of each of the communication links is analyzed for the communication architecture composed of two areostationary satellites, the colonies on Mars and Phobos, two cycler vehicles and the ground stations on Earth. Power requirements, antenna sizes and frequency are estimated for a demanding HDTV transmission from Mars and Phobos to Earth.

Table of Contents

List of Figures

Page

List of Tables

Page

1 Introduction

Earth-Mars cycler trajectories are a promising option for a transportation system from Earth to Mars in the context of a future human colonization mission to Mars. Earth-Mars cycler trajectories are Sun-centered orbits that periodically encounter both planets and could be used to send humans to Mars periodically and cost-efficiently, as the cycler vehicle (spacecraft in a cycler trajectory) remains in its orbit for an indefinite amount of time and could be used as the transportation infrastructure to Mars repeated times.

The existance of Earth-Mars cycler trajectories was first discovered by Rall [1] in 1969, and further summarized by Rall and Hollister [2] in 1971, identifying as well the possible existance of other kinds of cyclers. The cyclers found by Rall and Hollister are four-synodic-period cycler trajectories. In 1985, Aldrin [3] first suggested the existance of a single-synodic period cycler trajectory (Aldrin cycler), and Niehoff proposed the Versatile International Station for Interplanetary Transport (VISIT) 1 and VISIT 2 cyclers [4–6], which were further investigated and compared to the Aldrin cycler by Friedlander et al. [7] in 1986. The existance of the Aldrin cycler was confirmed by Byrnes et al. [8] in 1993. From 2002 to 2005, several new cyclers were identified by Byrnes et al. [9], Chen et al. [10–12] and McConaghy et al. [13, 14].

A cycler trajectory of particular interest is the so-called ballistic Earth-Mars S1L1 cycler trajectory (first identified in 2002 and further analyzed until 2006 by McConaghy et al. [13–16]). The ballistic S1L1 cycler is particularly promising as a future transportation system to Mars due to its relatively short Earth-Mars transfer times (for the outbound ballistic Earth-Mars S1L1 cycler trajectory) and low relative velocities with respect to the planets at the encounters. In addition, two outbound Earth-Mars S1L1 cycler vehicles launched one synodic period apart could be used to maximize the number of trips from Earth to Mars, as the S1L1 cycler trajectory is a two-synodic-period cycle, and the orbit opportunity appears every synodic period. In this study, the existance of the outbound ballistic Earth-Mars S1L1 cycler trajectory is verified in a circular-coplanar model.

Continuous and reliable communication from and to Mars will be required in a future human mission to Mars, and consequently, continuous coverage methods of Mars have become a research area of increasing interest since the late 1980s. Stevenson [17] first developed, in 1990, the requirements that need to be fulfilled by a Martian communication network, such as continuous time coverage, high-rate data transfer (for video and data services), and Mars-to-Earth, Mars-to-Phobos and Mars-Deimos communication links, among others.

Numerous Mars communication networks have been devised, such as halo orbit communication networks (first suggested by Pernicka et al. [18], 1992), areosynchronous networks (first introduced by Palamarick et al. [19], 1989), common-period four-satellite networks (developed by Draim [20] in 1987 for continuous Earth coverage, but also applicable to Mars as shown by Draim [21], 1991, and Danehy [22], 1997), multiple low-Mars orbit networks (studied by Hopkins [23], 1988, for Earth coverage), individually-dedicated communication orbiter-lander networks (traditional approach in planetary exploration) and networks with Martian landers on Phobos and Deimos (proposed by Hamilton [24], 1994). These Mars communication network designs were conveniently summarized and compared by Tai [25] in 1998.

More recently, researchers have focused on the optimization of satellite constellations in terms of the number of satellites for continuous and complete coverage of Mars. New and innovative methods for a Martian communication network consider the use of flower constellations (introduced by Mortari et al. [26], 2004, and applied to Mars by De Sanctis et al. [27] in 2007), or non-Keplerian orbits (first proposed by McKay et al. [28] in 2009 for Mars exploration). Interest has also grown in the development of communication architectures for communication, not only from and to the vicinity of the Earth, the Moon or Mars, but also from and to outer planets (Jupiter, Saturn, Neptune) or beyond within the Solar System (Bhasin et al. [29], 2004).

In this study, a novice method to provide an alternative Earth-Mars communication link over periods of Earth-Mars solar conjunction, by relaying the signal from and to Mars through the cycler vehicles, is proven to be possible (in a circular-coplanar model and in an ephemeris model); and two two-satellite Mars-centered communication constellations are designed (and compared), in a circular-coplanar model, to provide a continuous communication link

(but not complete coverage of the Martian surface) between human colonies on Phobos and Mars, and the Earth, in the context of a future Mars colonization mission with permanent human settlements on Mars and Phobos (inside Stickney Crater), and two outbound Earth-Mars S1L1 cycler vehicles as the human transportation system to Mars. The link performance of each of the communication links is analyzed for the communication architecture of the mission: two areostationary satellites, the colonies on Mars and Phobos, two cycler vehicles and the ground stations on Earth. Power requirements, antenna sizes and frequency are also estimated for an HDTV transmission (to account for a very demanding case) from Mars and Phobos to Earth.

Such a mission was proposed by Aldrin [30] in 2013, and was extensively studied by a 51-student team at Purdue University in Spring 2015, in collaboration with Dr. Buzz Aldrin, Dr. James Longuski, Sarag Saikia (Mission Design Advisor), and Peter Edelman (Teaching Assistant): Project Aldrin-Purdue. The contribution of the author, as part of the Mission Design Team, to Project Aldrin-Purdue (and additional work) is here explained in detail.

2 Circular-Coplanar Model of the S1L1 Cycler Trajectory

The procedure followed to verify the existance of the ballistic Earth-Mars S1L1 cycler trajectory described by the cycler vehicles is now developed in detail, in a circular-coplanar model.

2.1 Main Assumptions

The main assumptions of the circular-coplanar model are:

1. Earth and Mars perform circular orbits around the Sun.
2. Orbits of Earth, Mars and cycler vehicle lie in the ecliptic plane.
3. The cycler vehicle performs gravity-assist maneuvers only at the encounters with Earth: the cycler will encounter Mars, but the encounter will not change its orbit.
4. One synodic period is approximated and assumed to be equal to $2\frac{1}{7}$ years.
5. The distance from the Earth to the Sun, $r_{\oplus}$, is defined equal to one astronomical unit (AU): $r_{\oplus} = 1\ AU$.

Based on assumptions (4, 5), and given the definition of a synodic period, S, the distance from Mars to the Sun, $r_{\male}$, is computed from:

$$S = \frac{2\pi}{n_{\oplus} - n_{\male}}, \tag{2.1}$$

where $n_{\oplus} = \sqrt{\frac{\mu}{a_{\oplus}^3}}$ and $n_{\male} = \sqrt{\frac{\mu}{a_{\male}^3}}$ are the mean motions of the Earth and Mars, respectively (μ being the gravitational parameter of the Sun, $a_{\oplus} = r_{\oplus}$ and $a_{\male} = r_{\male}$ as the orbits of the planets are assumed to be circular).

The distance from Mars to the Sun is then calculated and assumed to be $r_{\male} = 1.5206\ AU$.

2.2 Given Information

Given that the trajectory described by the cycler vehicle is a S1L1 cycler trajectory, the problem under study is basically two coupled Lambert's problems where two orbits around the Sun need to be determined.

The known characteristics of the cycler trajectory are [16]:

1. Cycler vehicle performs a two synodic period cycle around the Sun.
2. Cycle is composed of two legs (an outer and an inner leg), and so two Lambert's problems need to be solved.
3. The apohelion of the outer leg needs to be larger than the distance from Mars to the Sun, so that the cycler vehicle can encounter Mars.
4. Initial position of the cycler vehicle coincides with the position of the Earth at that particular moment: as if the cycler had just encountered the Earth, or as if it had just launched from Earth.
5. After a time τ, the cycler vehicle encounters with Earth again, after performing at least one complete orbit around the Sun in its outer leg.

6. The cycler vehicle encounters with Earth again after a time: $4\frac{2}{7}$ years$-\tau$ after the previous encounter with Earth (the complete cycle is two synodic periods: $4\frac{2}{7}$ years), after performing at least one complete orbit around the Sun in its inner leg.

The S1L1 cycler trajectory, at the same time, is known to minimize the following [16]:

7. Relative velocities with respect to Earth and Mars at the encounters with the planets, in order to ease the rendezvous of the landers with the cyclers at the Earth's flyby, and to ease the establishment of the cycler in its orbit, as well as the entry, descend and landing (EDL) procedures on Mars.
8. TOF from Earth to Mars, in order for the crew that is sent to Mars not to spend an excessive amount of time on the cyclers (i.e. excessive in terms of bone loss effects, radiation exposure and supplies while in orbit).
9. ΔV required to switch from the outer to the inner leg, and vice versa (ΔV is, ideally, zero).

2.3 Analysis

2.3.1 Lambert's Problem

Based on points (1–5) in Sec. 2.2 and assuming Earth is at the position $\vec{r}_{\oplus,0} = \left[r_{\oplus}, 0\right]$ at the beginning of the cycle (right-handed coordinate system with origin centered at the Sun, x-axis points towards the initial position of the Earth and z-axis is parallel to the angular momentum vector of Earth and Mars), the Lambert's problem for the outer leg is completely defined by:

– Initial position: $\vec{r}_0 = \vec{r}_{\oplus,0} = \left[r_{\oplus}, 0\right]$.
– Final position: $\vec{r}_f = \vec{r}_{\oplus,\tau} = r_{\oplus}\left[\cos(n_{\oplus}\tau), \sin(n_{\oplus}\tau)\right]$.
– $TOF = \tau$.

Considering now also point (6) in Sec. 2.2, the second Lambert's problem for the inner leg is defined by:

– Initial position: $\vec{r}_0 = \vec{r}_{\oplus,\tau} = r_{\oplus}\left[\cos(n_{\oplus}\tau), \sin(n_{\oplus}\tau)\right]$.
– Final position: $\vec{r}_f = \vec{r}_{\oplus,4\frac{2}{7}} = r_{\oplus}\left[\cos(2\pi\frac{2}{7}), \sin(2\pi\frac{2}{7})\right]$.
– $TOF = 4\frac{2}{7}$ years $- \tau$.

The Lambert's problem solutions for elliptic orbits, which are the type of orbit performed by the cyclers around the Sun, are well-known and defined, depending on the type of elliptic orbit (1A, 1B, 2A or 2B), as [31]:

$$\sqrt{\frac{\mu}{a^3}}TOF = 2\pi R + \begin{cases} \left(\alpha_0 - \sin(\alpha_0)\right) - \left(\beta_0 - \sin(\beta_0)\right) & \text{for type 1A} \\ 2\pi - \left(\alpha_0 - \sin(\alpha_0)\right) - \left(\beta_0 - \sin(\beta_0)\right) & \text{for type 1B} \\ \left(\alpha_0 - \sin(\alpha_0)\right) + \left(\beta_0 - \sin(\beta_0)\right) & \text{for type 2A} \\ 2\pi - \left(\alpha_0 - \sin(\alpha_0)\right) + \left(\beta_0 - \sin(\beta_0)\right) & \text{for type 2B} \end{cases}, \tag{2.2}$$

where $TOF = \tau$ for the outer leg, and $TOF = 4\frac{2}{7} - \tau$ for the inner leg (τ in years), R is the number of complete revolutions around the central body performed during the TOF (in this case, $R = 1$, based on points (5, 6) in Sec. 2.2), $\alpha_0 = 2\sin^{-1}\left(\sqrt{\frac{s}{2a}}\right)$ and $\beta_0 = 2\sin^{-1}\left(\sqrt{\frac{s-c}{2a}}\right)$, where c is the distance from the initial to the final position of the Lambert's problem, and $s = \left(c + r_0 + r_f\right)/2$ is the semiperimeter of the space triangle (see Fig. 2.1) defined by the

position of the Sun, $\vec{r}_{\odot} = [0, 0]$ (at the origin), and the initial and the final positions of the Lambert's problem. The two Lambert's problems can then be solved (i.e. a solution for the semimajor axis a of the two orbits can be found) as the space triangles are completely defined by the initial and final positions as a function of TOF.

Figure 2.1 below is a representation of a generic space triangle of a Lambert's problem with initial position $\vec{r}_0$ and final position $\vec{r}_f$ with respect to a central body at the origin 0:

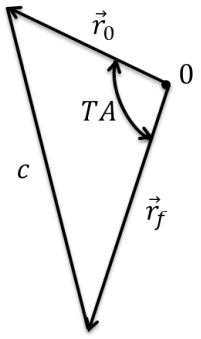

Figure 2.1: Generic Space Triangle

The transfer angle, TA, in the current analysis is easily related to TOF as $TA = n_{\oplus} TOF$.

Based on Sec. 2.2, the semimajor axes of the outer and inner legs of the cycle can be computed as a function of TOF, but first, the type of elliptic orbit (1A, 1B, 2A or 2B) needs to be determined.

By definition:

$$TA < \pi \text{ for type 1 orbit,}$$
$$\text{and } TA > \pi \text{ for type 2 orbit.}$$

In order to determine whether the type of the orbit is A or B, the TOF is compared to the TOF of the minimum energy transfer between the initial and final positions, TOF_{min}:

$$TOF_{min} = \frac{a_{min}^{3/2}}{\sqrt{\mu}} \left[2\pi R + \left(\alpha_{min} - \sin(\alpha_{min}) \right) - \left(\beta_{min} - \sin(\beta_{min}) \right) \right], \tag{2.3}$$

where $a_{min} = s/2$, $\alpha_{min} = 2\sin^{-1}\left(\sqrt{\frac{s}{2a_{min}}}\right)$ and $\beta_{min} = 2\sin^{-1}\left(\sqrt{\frac{s-c}{2a_{min}}}\right)$.

By definition:

$$TOF < TOF_{min} \text{ for type A orbit,}$$
$$\text{and } TOF > TOF_{min} \text{ for type B orbit.}$$

Once the semimajor axis of the orbit is computed, the semilatus rectum is computed, depending on the type of the elliptic orbit, as:

$$p = max\left(\frac{4a(s-r_0)(s-r_f)}{c^2} \sin^2\left(\frac{\alpha_0 \pm \beta_0}{2} \right) \right) \text{ for orbits 1A and 2B,} \tag{2.4a}$$

$$\text{and } p = min\left(\frac{4a(s-r_0)(s-r_f)}{c^2} \sin^2\left(\frac{\alpha_0 \pm \beta_0}{2} \right) \right) \text{ for orbits 1B and 2A.} \tag{2.4b}$$

Once the semimajor axis and semilatus rectum of the orbit are computed, the orbit is already completely defined.

2.3.2 The Ballistic S1L1 Cycler Trajectory

In order to minimize the ΔV required to switch from the outer to the inner legs, and vice versa, a gravity-assist maneuver is performed at the Earth encounters, which, ideally, will require no ΔV to switch between the orbits (definition of a ballistic cycler trajectory). A hyperbolic flyby can provide a change in the direction of the velocity of the cycler vehicle, however, the relative velocities with respect to Earth before and after the encounter cannot be modified by this gravity-assist maneuver. In this way, one of the conditions to switch between the outer and inner legs with no propulsive maneuver is that the relative velocities with respect to Earth in the outer leg and in the inner leg (i.e. right before and right after the encounter), need to be the same. Therefore, it is convenient to compare the relative velocities with respect to Earth of both legs at the Earth encounter as a function of TOF, in order to find the TOF corresponding to a ballistic cycler trajectory.

In Fig. 2.2, $V_{\infty/\oplus}$s are represented for both (outer and inner) legs as a function of τ in order to graphically identify what values of τ (recall that τ defines the TOFs of both legs) provide the same $V_{\infty/\oplus}$s for both legs, and consequently, to identify values of τ that will potentially yield a ballistic S1L1 cycler trajectory:

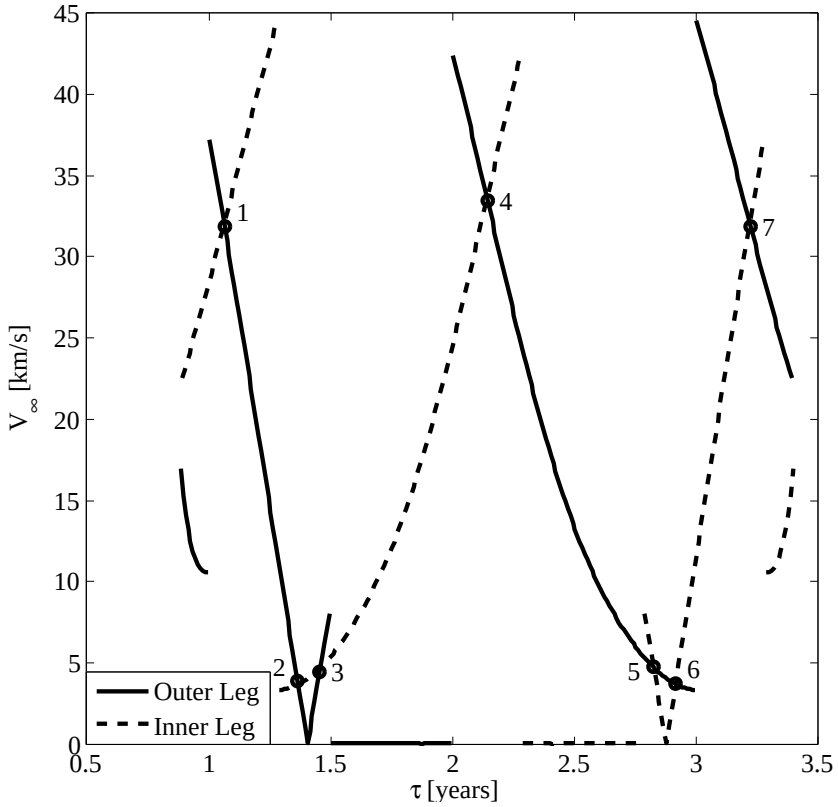

Figure 2.2: V_∞ at Earth Encounter as a function of τ

In Fig. 2.2, seven intersection points between the two lines (solid and dashed lines) can be identified. The seven values of τ that yield these intersection points are potential solutions for the ballistic S1L1 cycler trajectory as the relative velocities with respect to Earth of the outer and inner legs at the Earth encounter are the same, which would allow to switch between both legs without any propulsive maneuver.

It is worth to mention that the seven possible solutions found in Fig. 2.2 are symmetric with respect to $\tau = 2\frac{1}{7}$ years, due to the coupling in the TOFs of the two Lambert's problems. The solutions for $\tau < 2\frac{1}{7}$ years represent those solutions for which what was defined as "outer leg" would actually be the inner leg of the trajectory, and vice versa. The solution at $\tau = 2\frac{1}{7}$ years is such that the inner and outer legs are exactly the same orbit as the TOFs in both legs would be the same: $\tau = 2\frac{1}{7}$ years.

The discontinuities in V_∞ in Fig. 2.2 are due to a sudden change in the type of elliptic orbit (1A, 1B, 2A or 2B) described by the cycler for a particular value of τ; this sudden change in the type of orbit yields a discontinuity in the V_∞ at the Earth encounter as well.

For 1.5 years $< \tau <$ 2 years in Fig. 2.2, the V_∞ at the Earth encounter is zero, as the only solution for the Lambert's problem under study is, in fact, the orbit of the Earth. The physical meaning of such an orbit is that the cycler needs to perform the same orbit than the Earth (or to remain in a parking orbit around the Earth) in order to fulfill the conditions of the problem (Sec. 2.2); this, however, does not provide the desired solution as the cycler would not ever encounter Mars.

Further information about the resultant outer and inner legs is still required to determine if all the requirements of the cycler trajectory are fulfilled by these potential solutions.

In Fig. 2.3, the apohelion of the outer leg is represented in order to identify which of the previous seven potential solutions provide an apohelion sufficiently large for the cycler vehicle to encounter Mars:

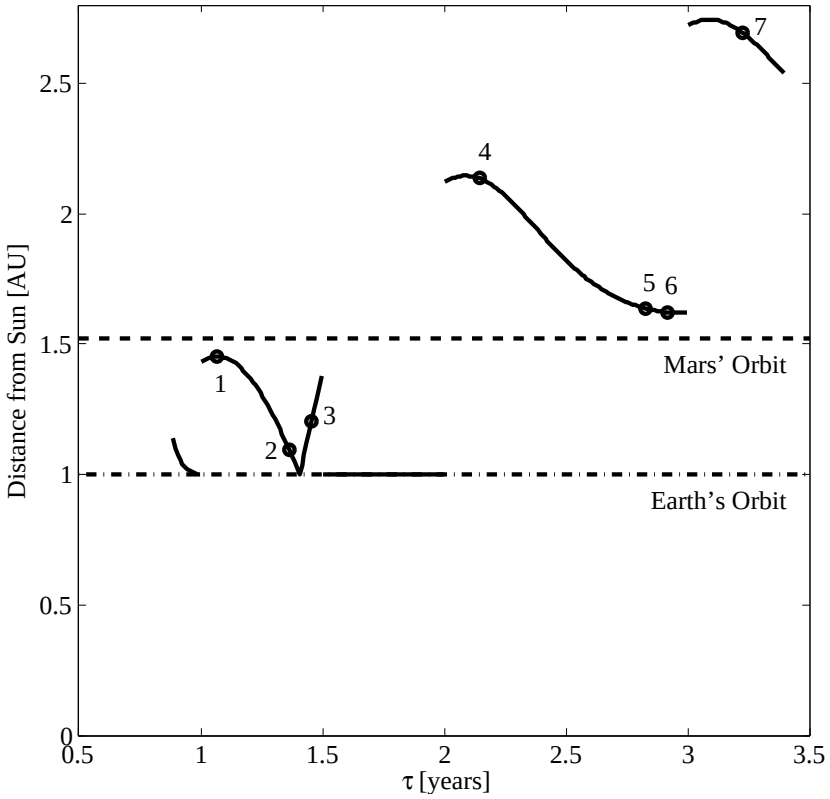

Figure 2.3: Apohelion of the Outer Leg as a function of τ

It can be observed in Fig. 2.3 that the apohelions of solutions 1 to 3 do not reach the orbit of Mars, therefore, these three solutions are not valid solutions for the outer leg (they do not fulfill point (3) in Sec. 2.2). The apohelion of solutions 4 to 7, instead, reach the orbit of Mars and therefore remain to be potential solutions for the ballistic S1L1

cycler trajectory.

Going back to Fig. 2.2, and considering that only solutions 4 to 7 could be solutions for the ballistic S1L1 cycler trajectory, it is noticed that solutions 5 and 6 provide minimum relative velocity with respect to Earth at the Earth encounter, $V_{\infty/\oplus}$, which is beneficial, both, to establish the orbit of the cycler and to rendezvous with the cycler when humans are sent to Mars.

Therefore, solutions 5 and 6 appear to be the two most promising solutions for the ballistic S1L1 cycler trajectory. In order to determine whether these solutions are actually ballistic or not, it needs to be verified if the Earth hyperbolic flyby can provide sufficient gravity assist to change the direction of the velocity of the cycler vehicle as required.

Figure 2.4 is a representation of a velocity diagram of a generic Earth hyperbolic flyby:

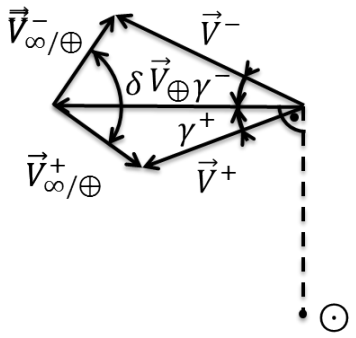

Figure 2.4: Velocity Diagram of a Generic Hyperbolic Flyby of Earth

In order to determine if a flyby can provide sufficient gravity assist for the S1L1 cycler trajectory to be ballistic, the maximum turning angle, δ_{max}, should be large enough (i.e. larger than the required turning angle, δ).

The turning angle required for the flyby, δ, is fully defined by the velocity and flight path angle prior to the encounter ($\vec{V}^-$ and γ^-, respectively, which are defined by the outer leg of the trajectory) and by the velocity and flight path angle after the encounter ($\vec{V}^+$ and γ^+, respectively, defined by the inner leg of the trajectory).

The maximum turning angle, δ_{max}, that can be achieved with the flyby is defined by the velocities with respect to Earth prior to the encounter, $\vec{V}^-_\infty$, and after the encounter, $\vec{V}^+_\infty$, together with the minimum possible perigee altitude (defined as $h_{min} = 200\ km$ to avoid interaction with the Earth's atmosphere): minimum perigee defines the minimum eccentricity of the hyperbola, e_{min}, which relates to the maximum turning angle as $\delta_{max} = 2\sin^{-1}\left(\frac{1}{e_{min}}\right)$.

If the turning angle analysis is performed for the potential solution 6, it is observed that the perigee required to generate the required turning angle lies below the surface of the Earth (i.e. $\delta_{max} < \delta$); therefore, the S1L1 cycler trajectory defined by solution number 6 is not ballistic.

The perigee altitude required for solution number 5, however, is found to be $h = 31818\ km > h_{min}$, as $\delta_{max} < \delta$.

In this way, solution number 5 (TOF between first and second Earth encounters, $\tau = 2.8276$ years) is found to be a ballistic S1L1 cycler trajectory, in a circular-coplanar model, as a flyby of Earth can provide sufficient gravity assist to switch between the outer and the inner legs of the trajectory without any propulsive maneuvers.

Table 2.1 summarizes the most relevant parameters of the ballistic S1L1 cycler trajectory just found:

Table 2.1: Ballistic S1L1 Cycler Trajectory Parameters

Leg	Semimajor axis [AU]	Eccentricity [-]	Argument of Periapsis [deg]
Outer Leg	1.3039	0.2554	-31.1
Inner Leg	1.0483	0.1609	20.4

Figure 2.5 is a representation of the ballistic Earth-Mars S1L1 cycler trajectory:

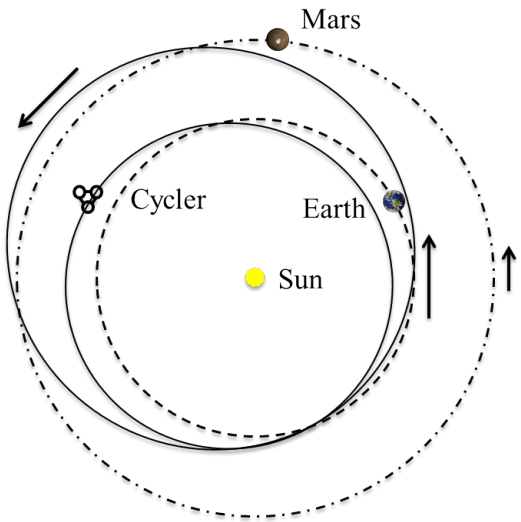

Figure 2.5: Ballistic Earth-Mars S1L1 Cycler Trajectory

The circular-coplanar model of the S1L1 trajectory provides a good estimate of TOF between the different encounters with Earth and Mars of the real orbits, and of the relative velocities with respect to Earth and Mars at the encounters with the planets. These estimations (see Table 2.2) will provide the reader an idea of the magnitude of TOFs and V_∞s of the S1L1 trajectory:

Table 2.2: Circular-Coplanar Estimations of TOF and V_∞

Leg	Encounters	TOF [days]	$V_{\infty/\oplus}$ [km/s]	$V_{\infty/\sigma}$ [km/s]
Outer Leg	Earth-Mars	154	4.71	4.99
	Mars-Earth	879	4.71	4.99
Inner Leg	Earth-Earth	533	4.71	N/A

Notice that the first Earth encounter (first row in Table 2.2) and the last Earth encounter (second Earth encounter in third row in Table 2.2) within a cycle represent the same flyby of Earth: at the very beginning and at the very end of that particular cycle. The velocity with respect to Earth at the Earth encounter, $V_{\infty/\oplus}$, is the same for the outer and inner legs as required for the ballistic S1L1 trajectory.

The same sequence of encounters (with the same characteristics) will be repeated every two synodic periods for all times.

The crew will travel from Earth to Mars between the Earth-Mars encounters (first row in Table 2.2), and therefore, humans will spend 154 days on the cycler vehicle. The TOF from Earth to Mars is not excessively long, which is convenient for the human factors part of the mission.

The S1L1 cycler trajectory, in the circular-coplanar model, is a ballistic trajectory, and therefore no propulsive maneuvers are required to maintain the cycler in its cycler trajectory, as the flybys of Earth can provide sufficient gravity assist to switch between the two legs of the trajectory.

The Earth-Mars S1L1 cycler trajectory was further analyzed by the Mission Design Team of Project Aldrin-Purdue in a more realistic ephemeris model (analysis was carried out in STOUR). The main conclusion of that analysis is that a ballistic S1L1 cycler trajectory is not possible: although a circular-coplanar model predicts its existance (the eccentricity and out-of-plane motion of the planets were neglected), in a more realistic model, minor trajectory correction maneuvers are required to keep the cycler in its orbit.

3 Cyclers as Communication Relays

The possibility to use the cycler vehicles as communication relays during Earth-Mars solar conjunction is considered to provide continuous communication between Earth and the colonies on Mars and Phobos. The analysis to prove that the cyclers can provide an alternative communication link during Earth-Mars solar conjunction is now described in detail.

The analysis is first performed in a circular coplanar model, and then the results are verified in an ephemeris model.

3.1 Main Assumptions

The circular-coplanar analysis is performed under the same assumptions listed in Sec. 2.1.

In addition to assumptions in Sec. 2.1, Fig. 3.1 can help to better understand the reasoning followed to determine whether communication between two bodies is possible:

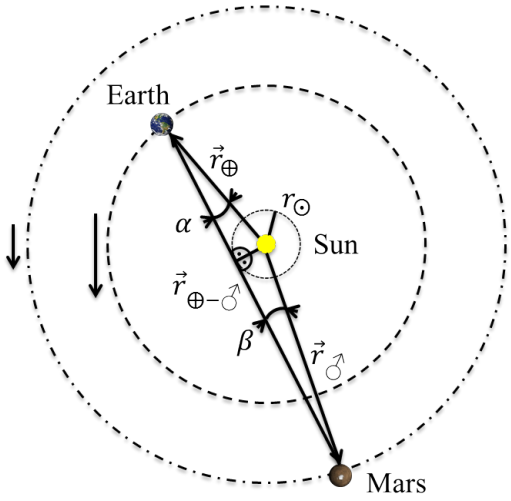

Figure 3.1: Communication Link before Solar Conjunction

Assume two bodies (in this case, Earth and Mars) whose distances with respect to the Sun are known ($r_{\oplus}$ and $r_{\sigma^{\prime}}$, respectively). Earth will be able to communicate with another body (in this case, Mars) only if the angle between $\vec{r}_{\oplus}$ and $\vec{r}_{\oplus-\sigma^{\prime}}$ is larger than the angle α illustrated in Fig. 3.1. The same applies to Mars, which will be able to communicate with Earth only if the angle between $\vec{r}_{\sigma^{\prime}}$ and $\vec{r}_{\oplus-\sigma^{\prime}}$ is larger than the angle β.

The limiting angles α and β for two arbitrary bodies can be computed if the distances from those two bodies and the Sun are known (in this case, $r_{\oplus}$ and $r_{\sigma^{\prime}}$) as $\alpha = \sin^{-1}\left(\frac{r_{\odot}}{r_{\oplus}}\right)$ and $\beta = \sin^{-1}\left(\frac{r_{\odot}}{r_{\sigma^{\prime}}}\right)$.

The radius $r_{\odot}$ that describes the sphere around the Sun inside which communication is not possible is determined to be $\alpha = 2.4^{\circ} - 2.7^{\circ}$ for the Earth [32].

In addition to the assumptions listed in Sec. 2.1:

6. The limiting angle α for Earth is assumed to be $\alpha = 3°$, to account for the error carried by the circular-coplanar model.

In this way, $r_{\odot}$ is then computed as $r_{\odot} = \sin(\alpha) r_{\oplus}$, with $r_{\oplus} = 1\ AU$.

3.2 Visibility Analysis

A visibility analysis between the Earth and Mars, between the Earth and the cyclers, and between Mars and the cyclers, is performed, both, in a circular-coplanar model and in an ephemeris model.

In order for the cyclers to be able to provide an alternative communication link during Earth-Mars solar conjunction, at least one of the cyclers should be visible from the Earth and Mars at the same time when the Earth, Mars and the Sun are aligned (Mars is nos visible from Earth, and vice versa).

3.2.1 Circular-Coplanar Model

The visibility analysis is performed by propagating along time the positions of Earth, Mars and the cyclers (based on the orbit parameters in Table 2.1), and by determining whether communication is possible or not at every timestep, based on the criteria described in Sec. 3.1.

Figure 3.2 is a representation of the availability of the communication links between Earth and Mars, between Earth, Cycler 1 and Cycler 2, and between Mars, Cycler 1 and Cycler 2, for the first three synodic periods after Cycler 1 is launched:

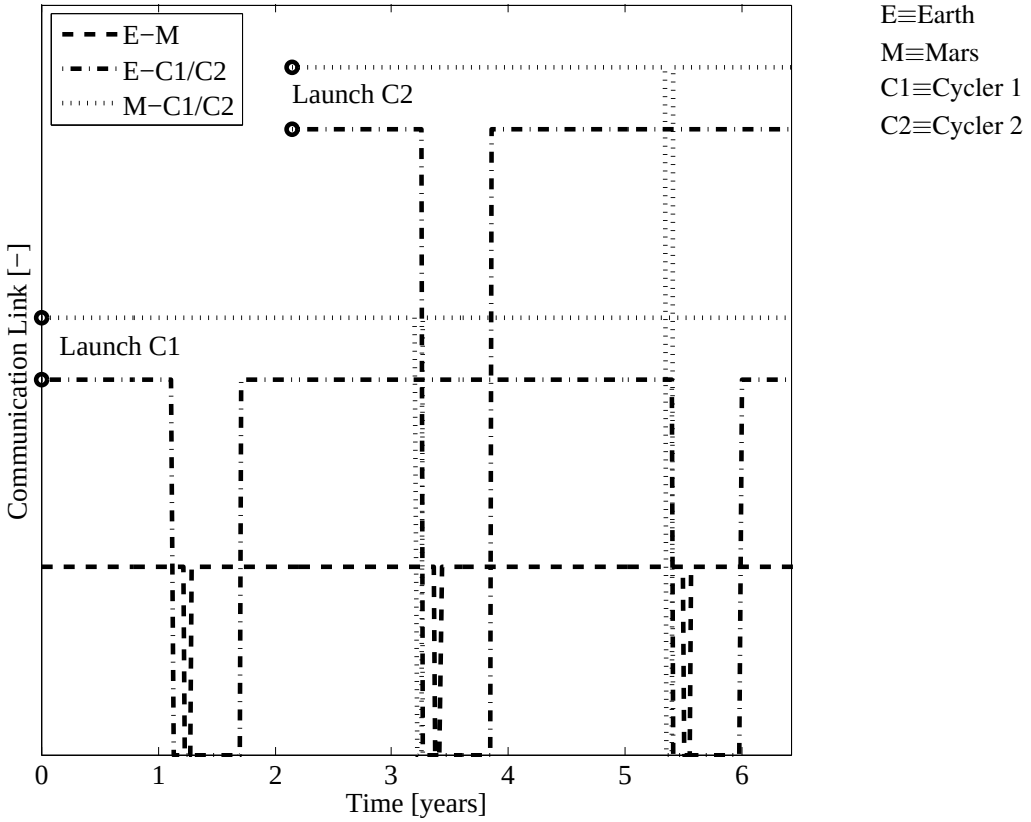

Figure 3.2: Communication Link Availability, Circular-Coplanar Model

Each horizontal line represents the availability of the direct communication link between two bodies. The gaps represent a solar conjunction between those two bodies, so that the direct communication link is not available due to the alignment of those two bodies and the Sun.

The dashed line represents the direct communication link between Mars and Earth. Solar conjunction occurs once every synodic period for ∼21 days (gaps in the dashed line at times $1\frac{1}{5}$ years, $3\frac{1}{4}$ years and $5\frac{1}{2}$ years, approximately). An alternative communication link should be provided by the cyclers at these times in order to maintain a continuous communication link between the Earth and the colonies on Mars and Phobos.

With only one cycler (Cycler 1) in orbit, an alternative communication link is not provided during the first Earth-Mars solar conjunction of a cycle ($4\frac{2}{7}$ years), as the Earth-Cycler 1 communication link is not available during the first Earth-Mars solar conjunction either (gap in the dash-dotted line corresponding to Cycler 1 at the same time there is a gap in the dashed line, at time $1\frac{1}{5}$ years). The same happens with Cycler 2 during the first Earth-Mars solar conjunction after its launch, at time $3\frac{1}{4}$ years (recall that Cycler 2 is launched $2\frac{1}{7}$ years after Cycler 1).

Once both cyclers are in orbit (both cyclers describe the same trajectory shifted $2\frac{1}{7}$ years in time), an alternative communication link during Earth-Mars solar conjunction is alternatively provided by the cyclers as they provide an alternative link during the second Earth-Mars solar conjunction of each cycle.

Figure 3.3 represents the availability of the communication links between Earth and Mars, between Earth, Cycler 1 and Cycler 2, and between Mars, Cycler 1 and Cycler 2, as Fig. 3.2 previously did. Now, the chosen communication link is also represented with a solid line:

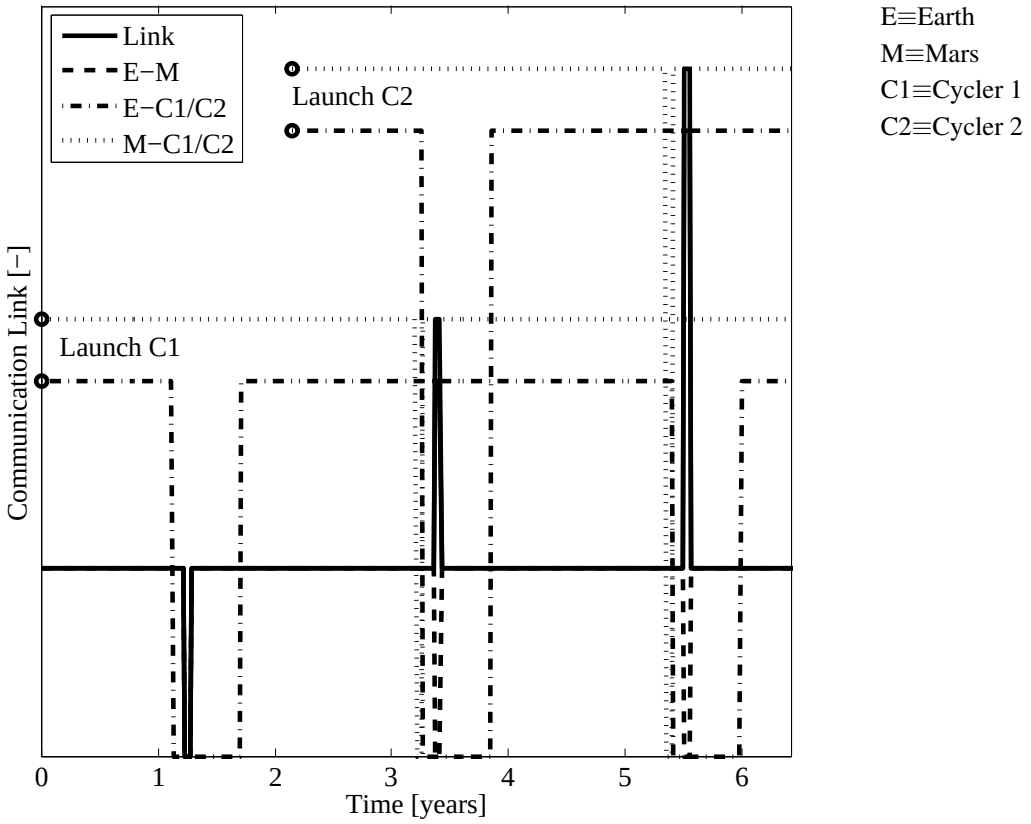

Figure 3.3: Continuous Earth-Mars Communication Link, Circular-Coplanar Model

The chosen communication link is the direct Earth-Mars communication link if available, and the alternative Earth-Cycler 1/Cycler 2-Mars communication link during Earth-Mars solar conjunctions.

The gap in the solid line at time $1\frac{1}{5}$ years represents the fact that only one cycler is not enough for continuous communication. Once both cyclers are in orbit (after Cycler 2 is launched), the cyclers alternatively provide an alternative communication link during Earth-Mars solar conjunction as the Earth-Cycler 1/Cycler 2 and Cycler 1/Cycler 2-Mars communication links are both available–dash-dotted and dotted lines do not present any gaps–during the second Earth-Mars solar conjunction of each cycle.

The main conclusion of this study is that, in a circular-coplanar model, two cyclers can provide an alternative communication link during every Earth-Mars solar conjunction (and only one cycler cannot), and so continuous communication between Earth and the colonies on Mars and Phobos can be achieved without the need of a heliocentric satellite communication network.

3.2.2 Ephemeris Model

The visibility analysis is performed by propagating the position of the cyclers along time based on the orbit parameters obtained from STOUR by the Mission Design Team of Project Aldrin-Purdue (STOUR provides orbit parameters and actual dates for the orbits of the cyclers), and recovering the positions of Earth and Mars from JPL Horizons (ephemeris model) for those specific dates. The visibility analysis is performed to determine if communication is possible or not at every timestep, based on the criteria described in Sec. 3.1.

Project Aldrin-Purdue will establish the orbits of the two cyclers in 2031 (Cycler 1) and 2034 (Cycler 2). Check-outs of the hyperbolic rendezvous with the cyclers will be performed by cargo in 2033 (with Cycler 1) and 2035 (with Cycler 2). The first crew will be sent to Mars in 2037 (on Cycler 1); therefore, both cyclers will be already in orbit (since 2034, after Cycler 2 is launched) when humans arrive to Mars in 2038. In principle, based on the results obtained in the circular-coplanar model in Sec. 3.2.1, continuous communication could be provided via the cyclers as both cyclers are already in orbit when humans first arrive to Mars.

Figure 3.4 represents the availability of the communication links between Earth and Mars, between the Earth, Cycler 1 and Cycler 2, and between Mars, Cycler 1 and Cycler 2, for the first two synodic periods after the first humans are sent to Mars on Cycler 1 in 2037:

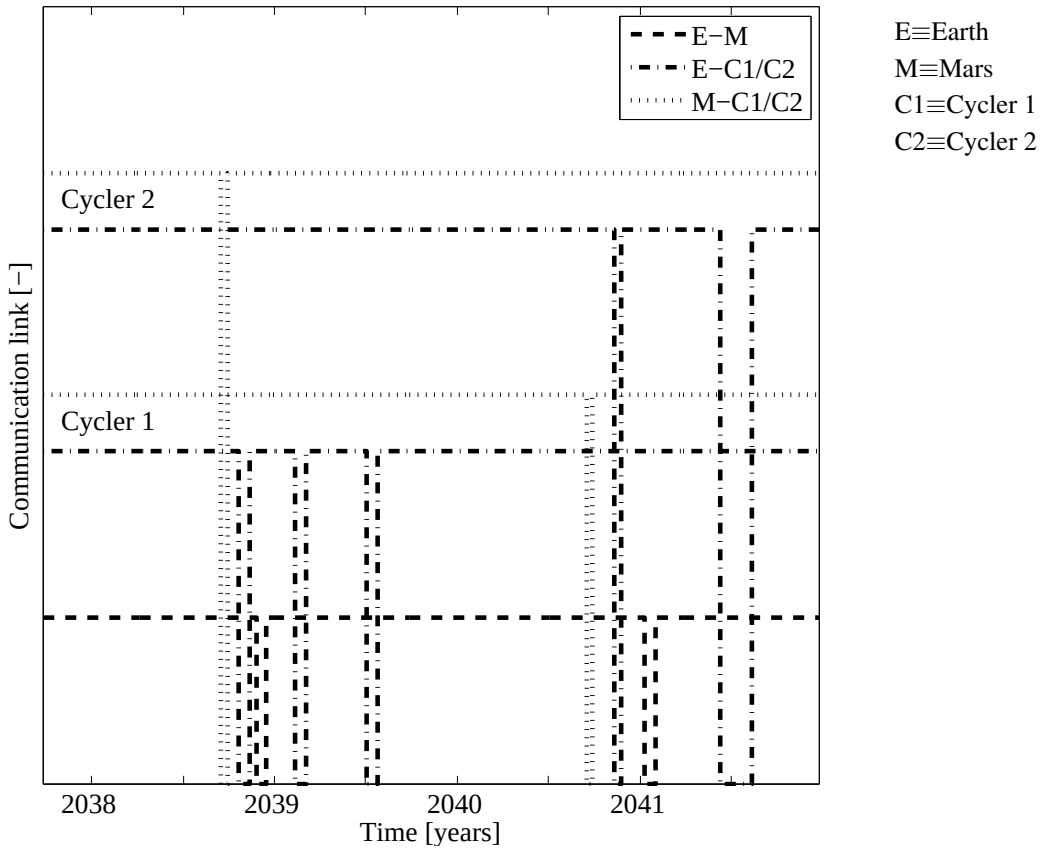

Figure 3.4: Communication Link Availability, Ephemeris Model

It is observed in Fig. 3.4 that Cycler 2 can provide an alternative communication link during the first Earth-Mars solar conjunction (at the end of 2038) after humans are sent to Mars, as Cycler 2 is already in orbit. During the second Earth-Mars solar conjunction (year 2041), Cycler 1 can provide an alternative link.

Figure 3.5 represents the chosen communication link that will provide continuous Earth-Mars communication (solid line):

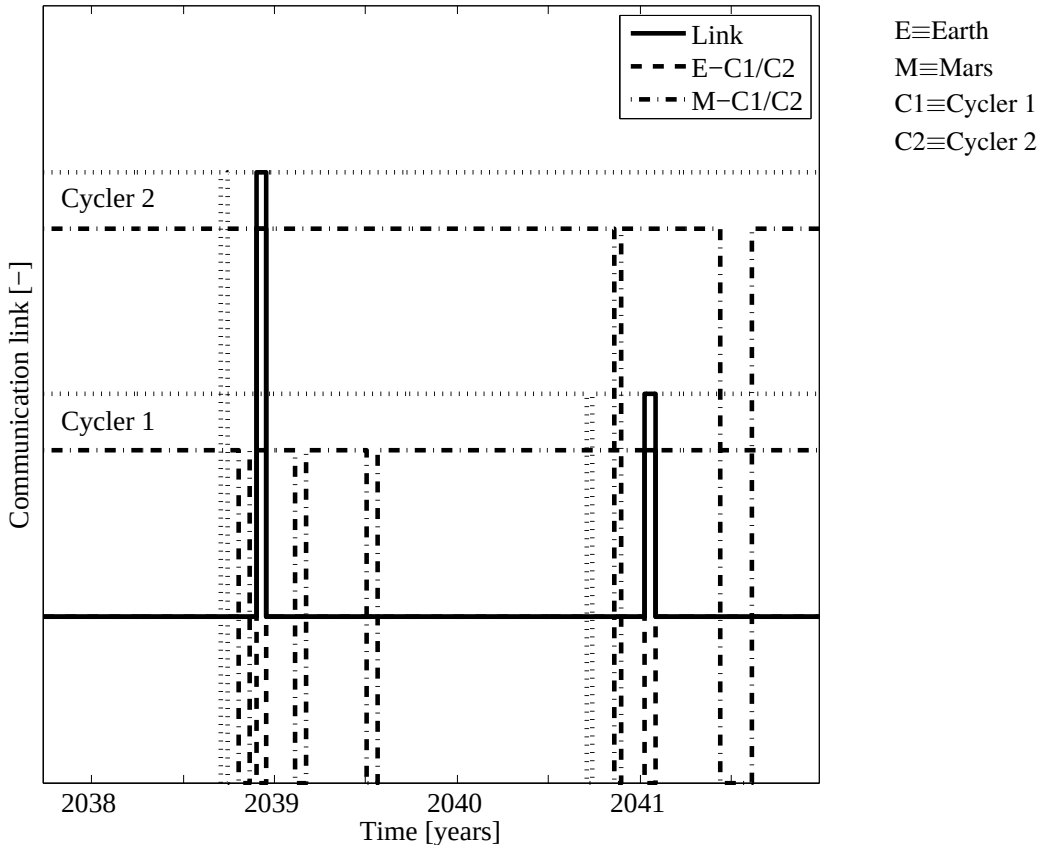

Figure 3.5: Continuous Earth-Mars Communication Link, Ephemeris Model

Therefore, it is proven, in an ephemeris model, that the cyclers are able to provide and alternative communication link during Earth-Mars solar conjunctions for continuous communication between Earth and the colonies on Mars and Phobos, during the first two synodic periods after the first humans are sent to Mars.

In these particular dates (first two synodic periods after first humans are sent to Mars), it is also observed that Cycler 1 can provide an alternative communication link during the first Earth-Mars solar conjunction too (at the end of 2038), as the Earth-Cycler 1 (dash-dotted line) and Mars-Cycler 1 (dotted line) links are both available during the first Earth-Mars solar conjunction. The same applies to Cycler 2, which is able to provide an alternative communication link during both Earth-Mars solar conjunctions of these particular two synodic period. One cycler was only able to provide and alternative link during the second solar conjunction of the cycle in a circular-coplanar model; in these particular two synodic periods, both cyclers can provide and alternative link during both Earth-Mars solar conjunctions. However, it cannot be assumed that a single cycler is enough to provide continuous communication, as, on a regular basis, each cycler will not be able to provide an alternative link during the first Earth-Mars solar conjunction of each cycle.

Continuous communication is expected and assumed to be possible for all times based on the results obtained in the circular-coplanar model (Sec. 3.2.1), and the analysis performed in an ephemeris model for the first complete cycle of Cycler 1 after the first humans are sent to Mars.

3.3 Communication Link Distance

The distance that the communication signal has to travel from Earth (direct or through a cycler) to Mars is relevant information for the link budget analysis and antenna sizing of the cyclers (see Sec. 5).

A circular-coplanar model is used–instead of an ephemeris model–to compute the communication link distance from Mars to Earth. The results obtained from the circular-coplanar model are a good estimate of the more realistic values that an ephemeris model would provide. An ephemeris model would yield slightly different communication distances every cycle (two synodic periods); the circular-coplanar model, however, provides periodic values (every two synodic periods) for the communication link distance, which could be interpreted as the averaged communication distance for all times.

Figure 3.6 represents the link distances corresponding to the possible communication links (direct Earth-Mars link, Earth-Cycler 1-Mars link and Earth-Cycler 2-Mars link) along the first three synodic periods after Cycler 1 is launched:

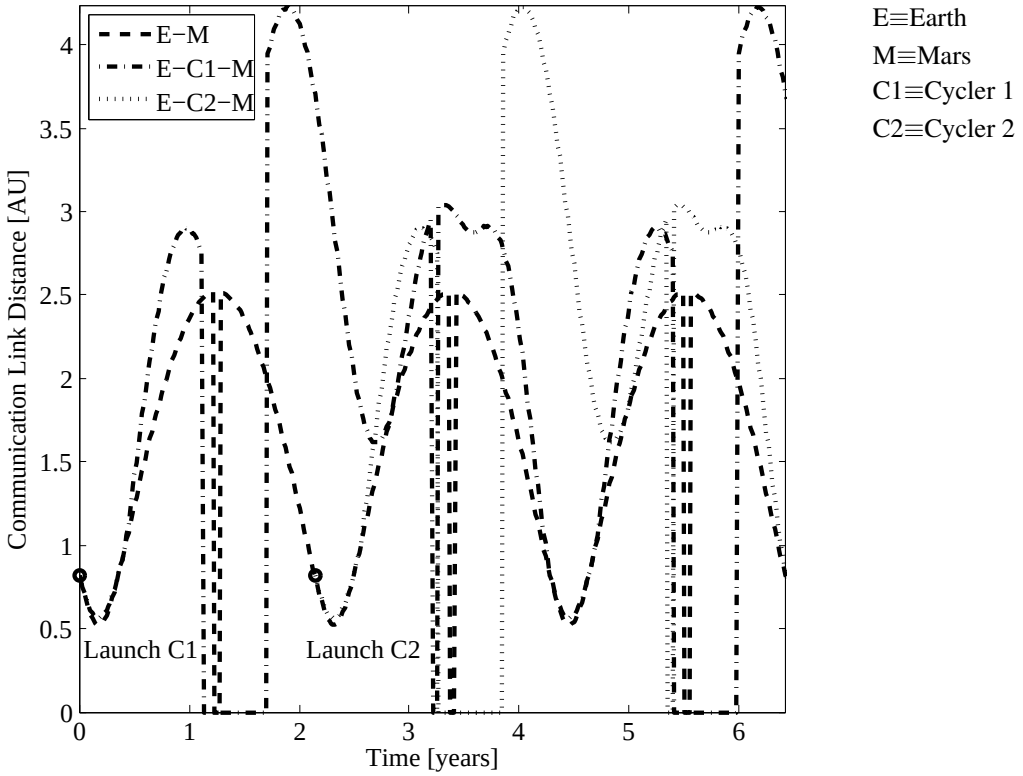

Figure 3.6: Possible Communication Link Distances

The gaps in the lines represent unavailability of the links (i.e. alignment of two bodies with the Sun); therefore, the Earth-Cycler 1-Mars communication link (dash-dotted line) will present gaps whenever there is an alignment between Earth, Cycler 1 and the Sun, or between Mars, Cycler 1 and the Sun. The same applies to the Earth-Cycler 2-Mars communication link (dotted line) and to the direct Earth-Mars communication link (dashed line).

The direct Earth-Mars communication link always provides the shortest link distance, and it is preferred for the same reason. The link provided by the cyclers is always larger than the direct Earth-Mars link as the signal has to

travel first from Earth to a cycler, and then from that particular cycler to Mars, instead of directly from Earth to Mars.

Figure 3.7 represents the communication link distance of the various available links, now including the chosen communication link that is used along time (i.e. direct Earth-Mars communication when available, and Earth-Cycler 1/Cycler 2-Mars during Earth-Mars solar conjunctions), with a solid line:

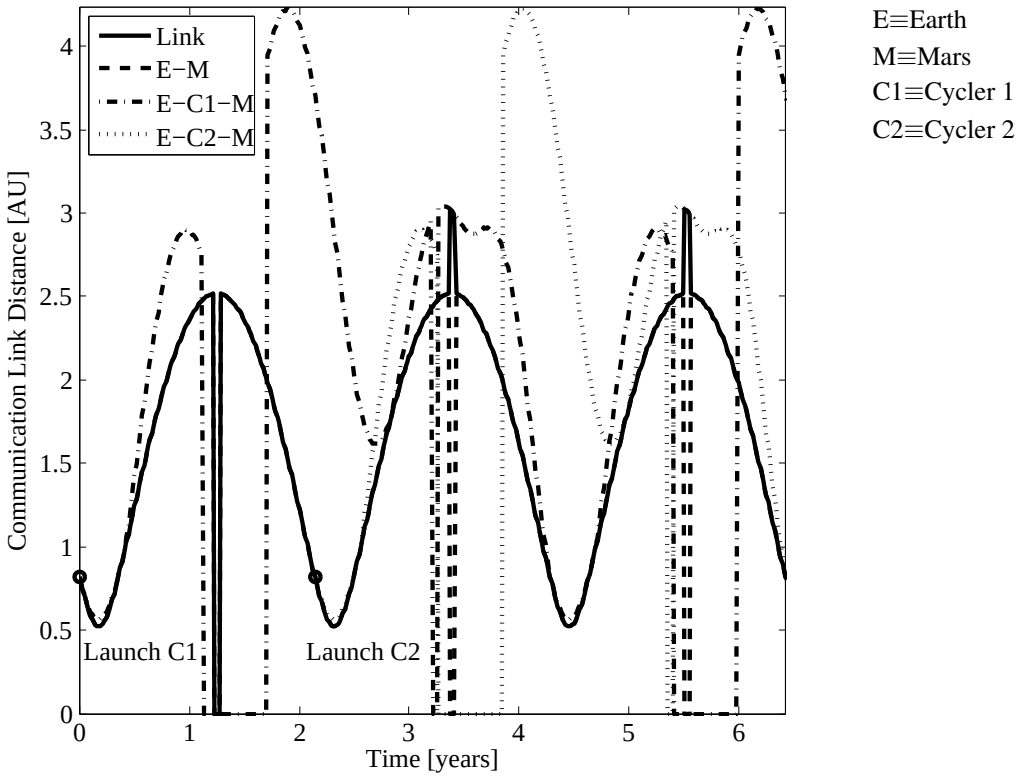

Figure 3.7: Continuous Earth-Mars Communication Link Distance

In Fig. 3.7, before Cycler 2 is launched (at time $2\frac{1}{7}$ years), it is observed again that Cycler 1 alone is not able to provide an alternative link during the first Earth-Mars solar conjunction (gap in the solid line at time $1\frac{1}{5}$ years) after Cycler 1 is launched, as the communication link provided by Cycler 1 (dash-dotted line) is not available either. Once both cyclers are in orbit, an alternative communication link is provided by one of the cyclers alternatively for every subsequent Earth-Mars solar conjunction: first, by Cycler 1 at time $3\frac{1}{4}$ years, and second, by Cycler 2 at time $5\frac{1}{2}$ years. The same communication strategy sequence can be repeated every subsequent cycle.

Fig. 3.8 is a representation of the link distance, in light-minutes (lm), from Mars to Earth (direct link or through the cycler vehicles) once the communication sequence is chosen (based on Fig. 3.7):

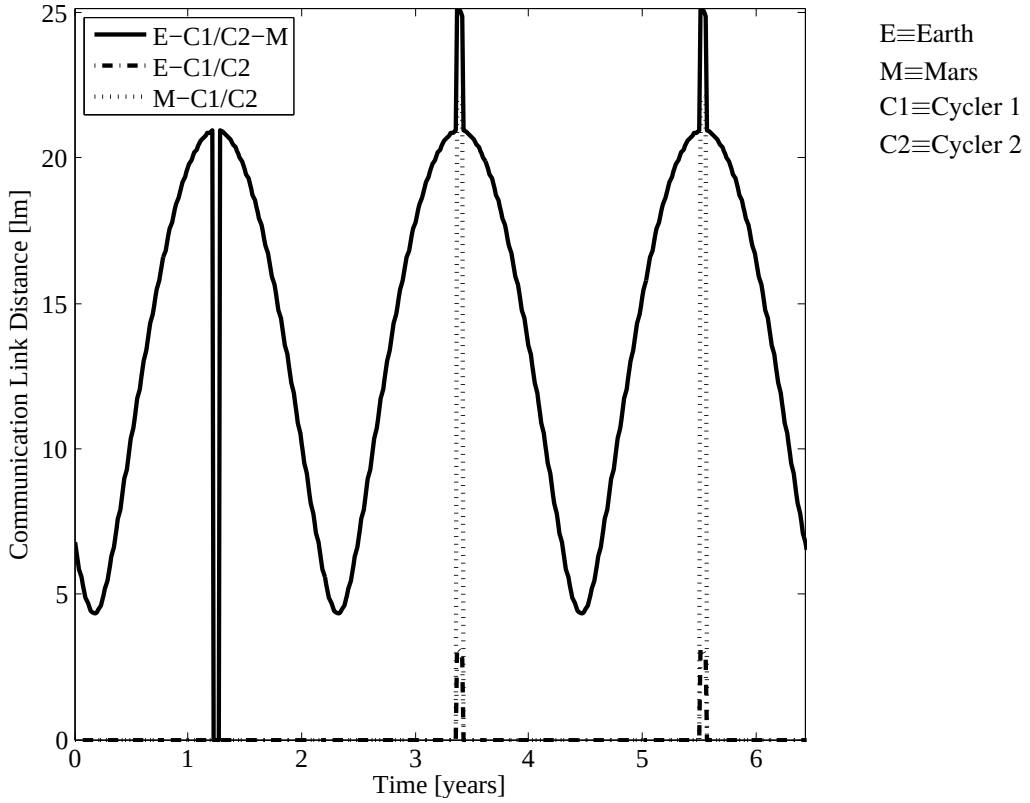

Figure 3.8: Communication Link Distance

The gap in the solid line at time $1\frac{1}{5}$ years represents the fact that only one cycler cannot provide an alternative communication link during all Earth-Mars solar conjunctions.

The dash-dotted and dotted lines represent the communication link distance from Earth to the Cycler 1/Cycler 2 and from the Cycler 1/Cycler 2 to Mars, respectively, when one of the cyclers is used to relay the signal from Mars to Earth; the addition of these two distances is equal to the total communication link distance when the cyclers relay the signal (solid line).

When the cyclers relay the signal from Mars to Earth (at time $3\frac{1}{4}$ years for Cycler 1, and $5\frac{1}{2}$ years for Cycler 2), the communication link distance is suddenly increased (jump in the solid line), which will cause a delay in the signal reception of 4 minutes. When the direct Earth-Mars link is recovered, the communication link distance is suddenly decreased (drop in the solid line); this will cause the direct signal between Earth and Mars to be received before the signal that was previously relayed by one of the cyclers (i.e. overlap in the signal reception), as this second signal has to travel a longer distance.

The delay in the reception of the signal should not represent a major issue; it will take place on a periodic basis (every synodic period), no information will be lost and it can be easily predicted.

One possibility to avoid the overlap in the signal reception is to keep communicating through the cycler until the direct Earth-Mars link distance and the Earth-Cycler 1/Cycler 2-Mars link distance are closer together. Observe in Fig. 3.7 that the link distance of the communication link provided by the cycler approaches the direct Earth-Mars link

distance after that particular cycler relayed the signal: Earth-Cycler 1-Mars link distance (dash-dotted line) approaches the direct Earth-Mars link distance (dashed line) at time $4\frac{1}{2}$ years after Cycler 1 relayed the signal, and Earth-Cycler 2-Mars link distance (dotted line) approaches the direct Earth-Mars link distance at the end of the third synodic period.

Another solution for the overlap in signal reception is to develop a software capable of holding the signal that is directly transmitted between Earth and Mars until the previously relayed signal by the cycler is fully recovered. Once the signal relayed by the cycler is fully received, the signal directly transmitted between Earth and Mars can be streamed again.

Table 3.1 summarizes the maximum communication link distance from one cycler to Earth and from that cycler to Mars (over the time that that particular cycler relays the signal from Mars to Earth), and the maximum communication distance from Mars to Earth. These maximum communication distances are relevant for the link budget analysis (Sec. 5) as they represent the most demanding case for these communication links:

Table 3.1: Maximum Communication Link Distances

Communication Link	Communication Link Distance [AU]
Cycler 1/Cycler 2-Earth	0.4
Cycler 1/Cycler 2-Mars	2.7
Mars-Earth	2.5

Notice in Table 3.1 than the link from the cyclers to Earth is much less demanding that the link from the cyclers to Mars.

4 Communications Satellite Constellation around Mars

The procedure followed to design the Mars-centered communications satellite constellation is now described in detail, in a circular-coplanar model.

4.1 Introduction

The Mars-centered satellite communication network required to maintain continuous communication between the colony on Mars, the colony on Phobos, and the Earth (or one of the cyclers) is now under study.

The colony on Phobos is placed inside Stickney Crater (Stickney Crater faces Mars, and Phobos is tidally locked to Mars). The visibility from inside the crater will be limited (maximum angular visibility, β), and determined by the geometry of the crater itself.

Figure 4.1 represents the problem under study, where communication between the colony on Phobos (orbiting around Mars), the colony on Mars (rotating around the rotational axis of Mars) and the Earth (or one of the cycler) needs to be provided for all times by means of a Mars-centered communications satellite constellation. Direct Phobos-Mars communication is preferred. If not available, the satellites should be able to relay the signal from Phobos to the colony on Mars. At the same time, the satellites should be able to communicate with Earth/Cycler 1/Cycler 2, both, the signals from Phobos and from Mars (the colonies on Phobos and Mars do no communicate directly with the Earth):

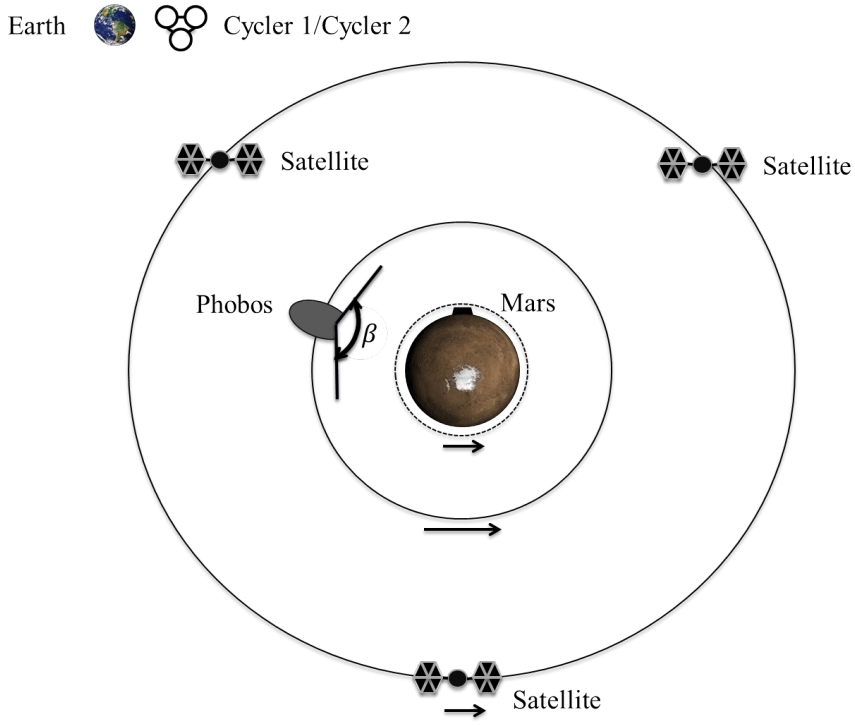

Figure 4.1: Communication Satellites around Mars for Continuous Communication

4.2 Main Assumptions

The main assumptions for the current analysis are:

1. Colony on Mars is at $\pm 5^\circ$ Latitude.
2. Colony on Phobos is inside Stickney crater. Maximum visibility (angle β) is determined based on the geometry of the crater [33]. This angle is found to be $\beta = 152^\circ$.
3. Phobos is in a circular orbit with zero inclination (actual values of eccentricity and inclination are 0.0151 and 1.093°, respectively) at an altitude $h_P = 5980$ km.
4. Communication between satellites and Phobos, or between satellites and Earth, is not possible if the signal has to travel through the atmosphere of Mars (120 km altitude).
5. Communication between the colony on Mars and the satellites, or Phobos, is not possible unless they are visible above a minimum elevation angle above the horizon $\varepsilon_{cr} = 5^\circ$ (equivalent maximum visibility angle β of 170° for the colony on Mars).

4.3 Proposed Solutions

Two possible solutions for the problem under study are proposed and compared. The most convenient solution is chosen as the final design for the mission (Sec. 4.7).

4.3.1 Two Communication Satellites in Phobos' Orbit

The first of the two possible solutions for the communications satellite constellation around Mars is now described.

Figure 4.2 represents the geometry of a satellite constellation composed of two satellites placed in Phobos' orbit, spread 120° apart from Phobos and from each other:

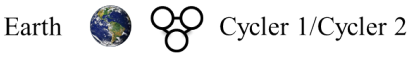

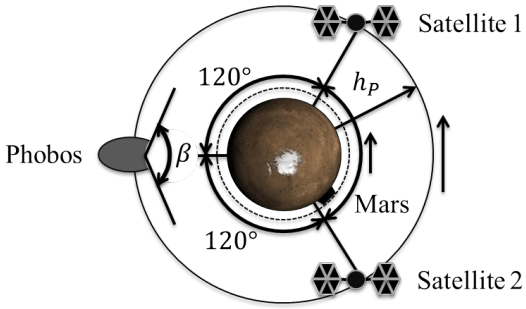

Figure 4.2: Geometry of Communications Satellite Constellation in Phobos' Orbit

This configuration is convenient as Phobos will always be able to communicate with the satellites, as their relative positions are conserved. Also, the colony on Mars will be able to communicate with at least one out of Phobos, Satellite 1 or Satellite 2, at all times. At least one of the communication satellites will be able to communicate with Earth (or one of the cyclers if the signal is relayed) as well.

Figure 4.3 is a representation of the communication links between Phobos and the satellites, and the communication link between one of the satellites (Satellite 2) and the colony on Mars. The communication link between one of the satellites (Satellite 1) and the Earth is represented as well:

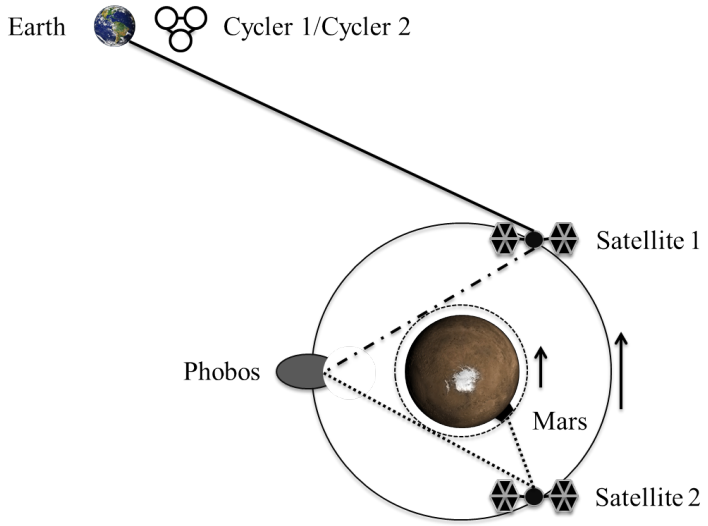

Figure 4.3: Communication Links of Communications Satellite Constellation, Phobos' Orbit

In Fig. 4.3, it can be seen how the signal from Phobos to Mars is relayed by Satellite 2 (dotted lines), so that communication is possible between Phobos and Mars. At the same time, Phobos can communicate information from Mars and Phobos to Satellite 1 (dash-dotted line), and Satellite 1 communicates this information to Earth (solid line).

4.3.2 Two Communication Satellites in an Areostationary Orbit

A second possible solution for the problem under study is now provided and described.

Figure 4.4 represents a satellite constellation composed of two satellites placed in an areostationary orbit (stationary orbit around Mars, altitude $h_S = 17032$ km), separated by an angular distance $\alpha = 65°$ (α is dependent on the latitude of the colony, see Sec. 4.6.2), and centered about the meridian that passes over the colony on Mars:

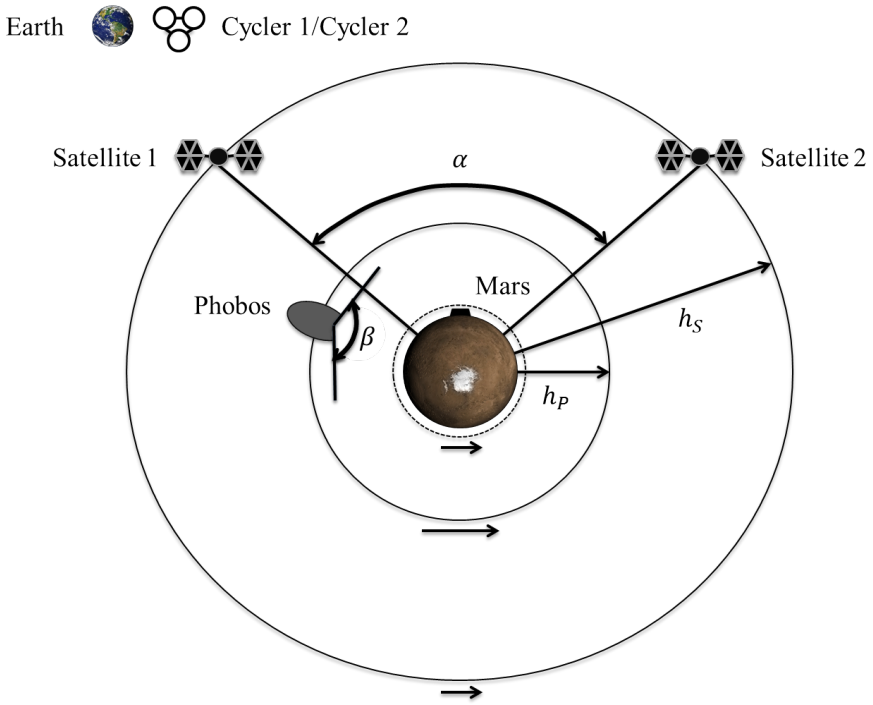

Figure 4.4: Geometry of Communications Satellite Constellation, Areostationary Orbit

This configuration is convenient as the colony on Mars will always be able to communicate with the satellites (their relative positions are conserved). At the same time, for all times, at least one of the satellites will be able to communicate with Earth due to the angular separation between them. In the same way, due to the angular separation between the satellites, Phobos will be able to communicate with at least one of them at all times.

Figure 4.5 represents the communication links between Phobos and one of the satellites (Satellite 2, dotted line), between the colony on Mars and the satellites (dash-dotted line for Satellite 1 and dotted line for Satellite 2); and the communication link between one of the satellites (Satellite 1) and the Earth is represented with a solid line:

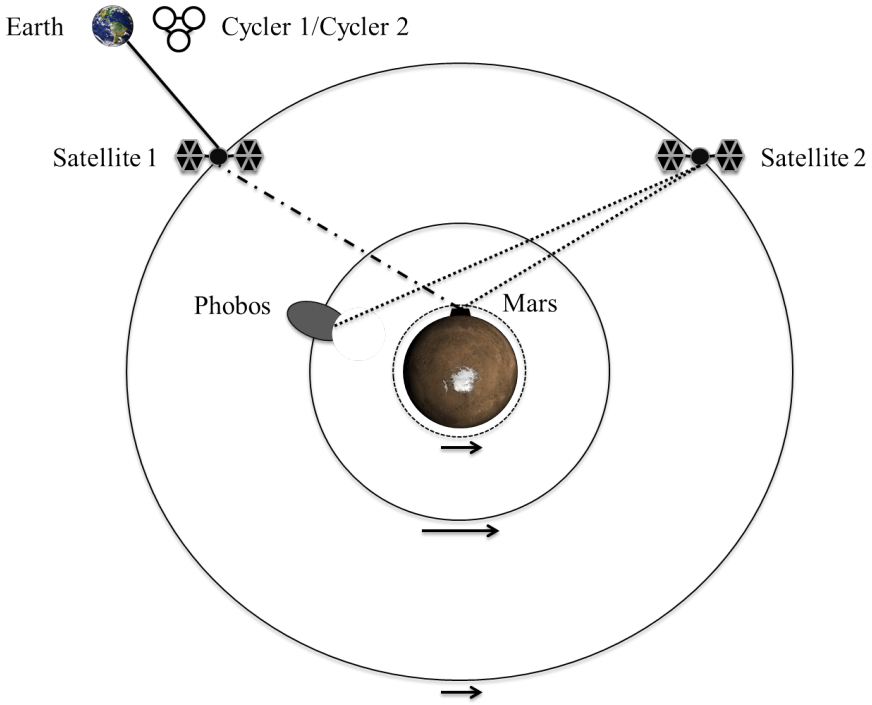

Figure 4.5: Communication Links of Communications Satellite Constellation, Areostationary Orbit

In Fig. 4.5, it can be seen now how the signal from Phobos to Mars is relayed by Satellite 2, so that communication is possible between Phobos and Mars. At the same time, Mars can communicate information from Phobos and from Mars to Satellite 1, and Satellite 1 communicates this information to Earth.

4.4 Visibility Analysis

A visibility analysis similar the analyses performed in Sections 3.2.1 and 3.2.2 is now performed for the two communications satellite constellations around Mars.

The same criteria as the criteria explained in Sec. 3.1 is used to determine whether communication is possible or not between the satellites, Phobos and Earth or a cycler; however, $r_{\odot}$ should be now replaced by the radial distance from the center of Mars to the top of the Martian atmosphere.

In order to determine whether communication is available between the colony on Mars and the communication satellites, or the colony on Phobos, consider the colony on Mars is placed at $0°$ Latitude, and consider a communication satellite at a radial distance r_c from the center of Mars (see Fig. 4.6):

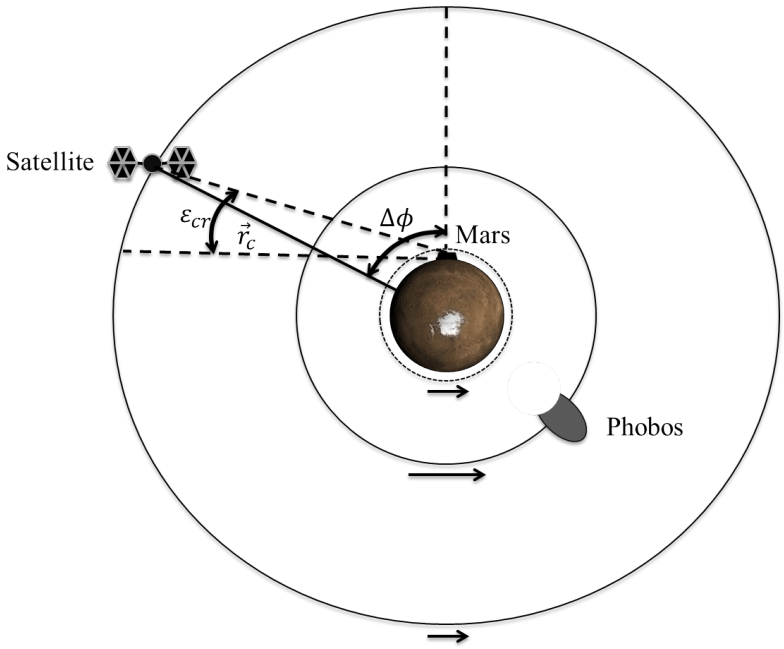

Figure 4.6: Minimum Elevation Angle and $\Delta\phi$ Configuration

The minimum elevation angle above the horizon at which the colony on Mars can communicate, ε_{cr}, determines the maximum longitude difference, $\Delta\phi$, above which communication would not be possible between the colony on Mars and the communication satellite.

The maximum value of $\Delta\phi$ for communication is dependent on the latitude of the colony, and once that value is computed for the particular latitude at which the colony is located, it is determined (by computing the longitude difference) for every timestep whether communication is possible or not between the colony and the communication satellites or the colony on Phobos.

4.4.1 Two Communication Satellites in Phobos' Orbit

The visibility analysis for the first of the two possible solutions for the communications satellite constellation around Mars is now performed.

Figure 4.7 is a representation of the availability of the communication link between the Earth (or one of the cyclers) and the satellites around Mars (dash-dotted line for Satellite 1, and dotted line for Satellite 2), during one Martian day (or sol: approximately, 24 hours and 37 minutes per Martian day). The communication link between a satellite and the Earth will be available unless the Earth, the satellite and Mars are aligned:

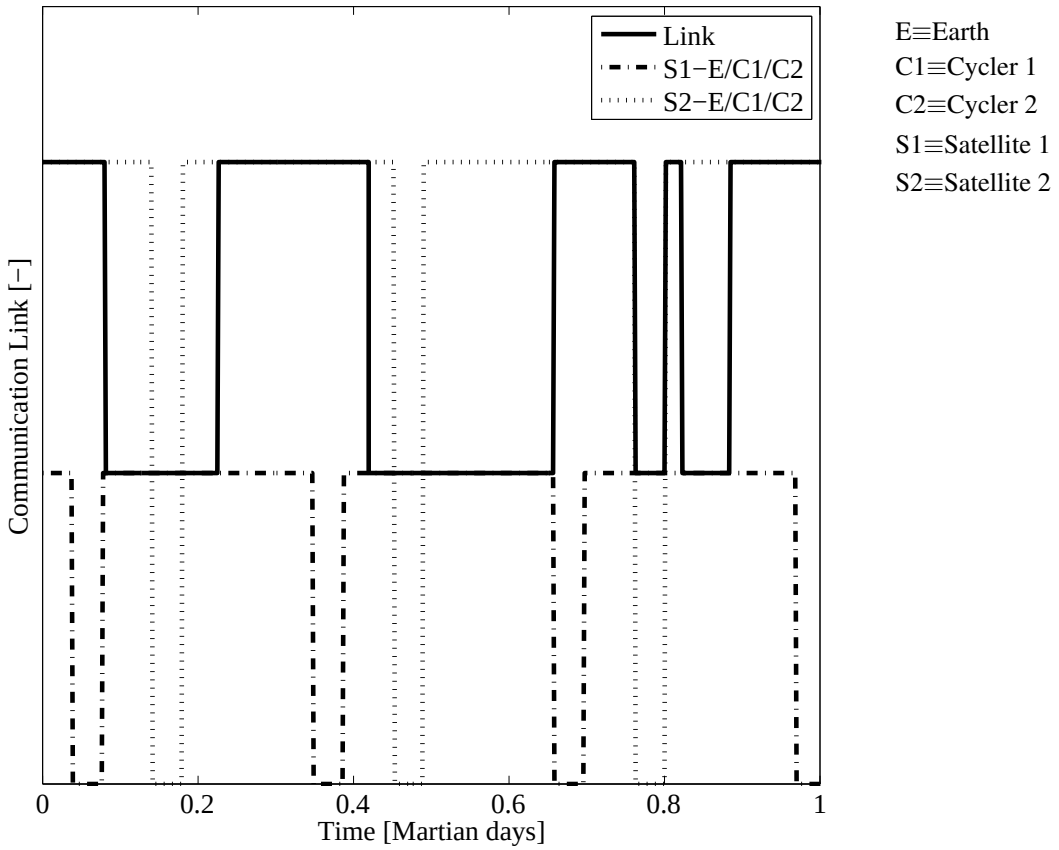

Figure 4.7: Availability of Communication Links from Satellites, Phobos' Orbit

For all times, there is at least one satellite that can communicate with the Earth: when Satellite 2 cannot communicate with Earth (gap in the dotted line), Satellite 1 can (no gaps in the dash-dotted line at that time), and vice versa.

The solid line represents which satellite is used to communicate with Earth over time, this sequence is determined by the availability of the communication links between Phobos and Mars, between the satellites and Mars, and between the satellites and Phobos.

Figure 4.8 is a representation of the availability of the communication link of the satellites and Phobos with the colony on Mars, during one sol:

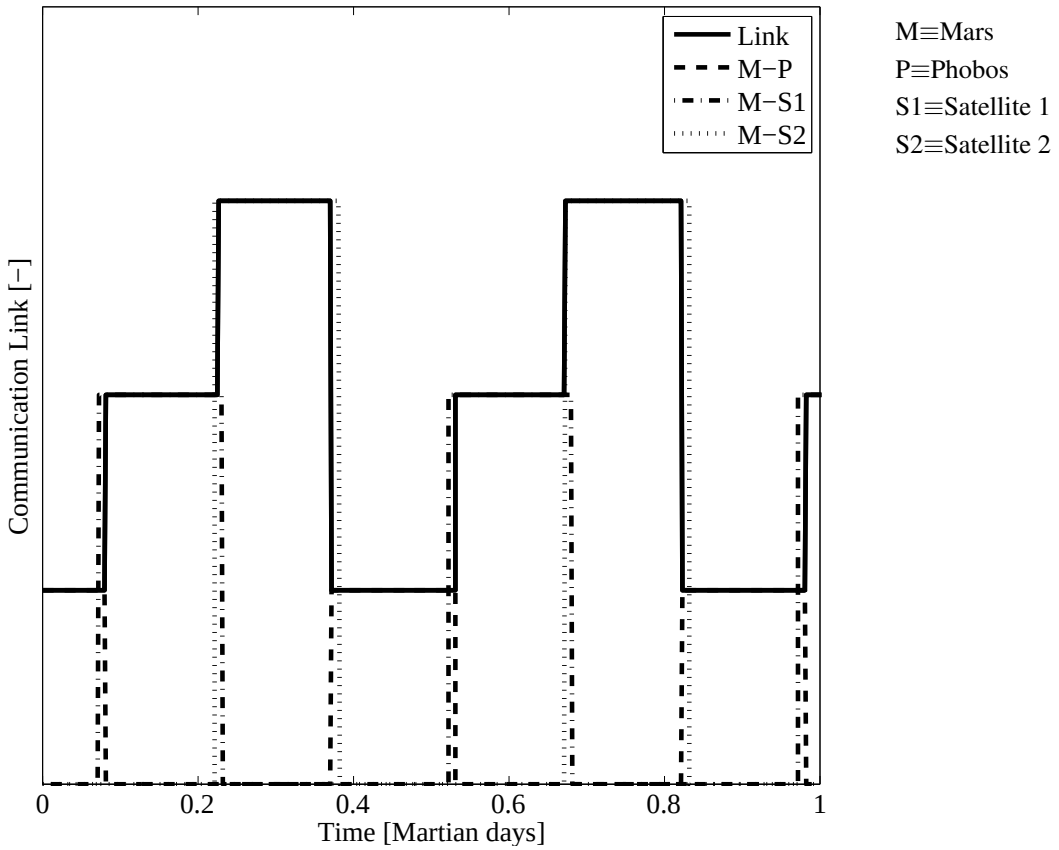

Figure 4.8: Availability of Communication Links from Mars, Phobos' Orbit

The communication link between the satellites and Phobos is periodic (every half a sol) and available for about $\frac{1}{3}$ of the time. The availability of the communication link of the colony on Mars with the satellites and Phobos follows the same behavior, but as the satellites and Phobos are spread 120° apart from each other in the same orbit, their availabilities are shifted in time. In this way, the colony on Mars, for all times, will be able to communicate with at least one out of these three bodies (satellites or Phobos).

The solid line represents the communication sequence followed by the colony on Mars: The colony on Mars will communicate only with one out of the three bodies (satellites or Phobos) at a time. If direct communication with Phobos is available, Mars will communicate with Phobos and Phobos will communicate with one satellite (this satellite should be able to communicate with the Earth). The colony on Mars will communicate with a satellite instead if Phobos is not visible, this satellite will communicate with both, Phobos and Earth, if the Earth is visible from that satellite; or the satellite will communicate with both, Phobos and the other satellite, for the signal to be relayed by that other satellite to Earth if the Earth is not visible from the first satellite.

Figure 4.9 is a representation of the availability of the communication links from Phobos to the satellites and to Mars, during one sol:

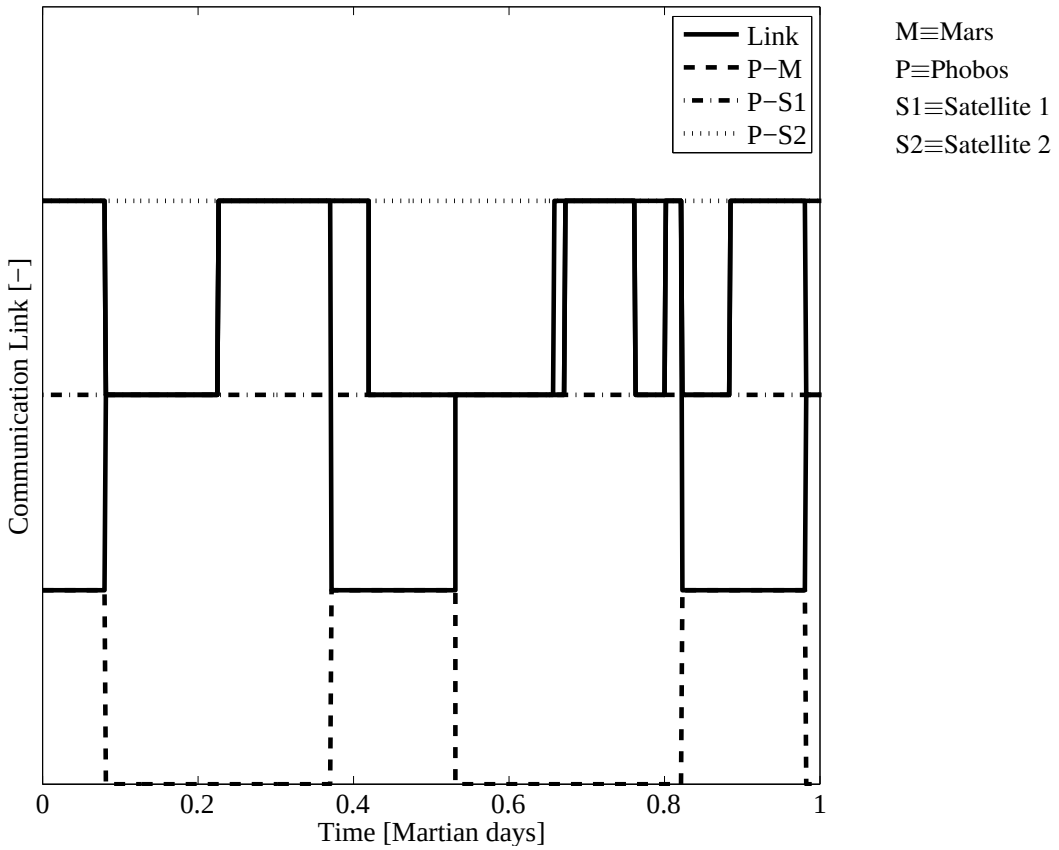

Figure 4.9: Availability of Communication Links from Phobos, Phobos' Orbit

It is observed in Fig. 4.9 that communication between the satellites and Phobos is always available (no gaps in the dash-dotted and dotted lines) as the relative positions between the three are conserved along time, due to the fact that the satellites are in the same orbit than Phobos. Communication between Phobos and the colony on Mars is periodically lost (every half a sol) for about $\frac{1}{3}$ of the time, due to the fact that Phobos orbits around Mars, and therefore, Phobos and the colony on Mars will eventually be on opposite sides.

The solid line represents the communication sequence followed by Phobos: Phobos will communicate directly with the colony on Mars when possible, and, at the same time, with the satellite that can communicate with Earth. If direct Phobos-Mars communication is not available, Phobos will communicate with one satellite and that satellite will relay the signal to Mars. Phobos will commmunicate only with one satellite if that same satellite can communicate at the same time with Earth and with the colony on Mars. Phobos will communicate at the same time with both satellites if the satellite that relays the signal to Mars cannot communicate with Earth (the other satellite will be able to communicate with Earth).

The main conclusion of this visibility analysis is that continuous communication between the colonies on Phobos and Mars, and the Earth, can be provided with only two satellites around Mars, if placed in the same orbit than Phobos.

4.4.2 Two Communication Satellites in an Areostationary Orbit

The visibility analysis for the second proposed solutions is now performed and explained in detail.

Figure 4.10 is a representation of the availability of the communication link between the satellites around Mars (dash-dotted line for Satellite 1 and dotted line for Satellite 2) and the Earth (or one of the cyclers), during one sol:

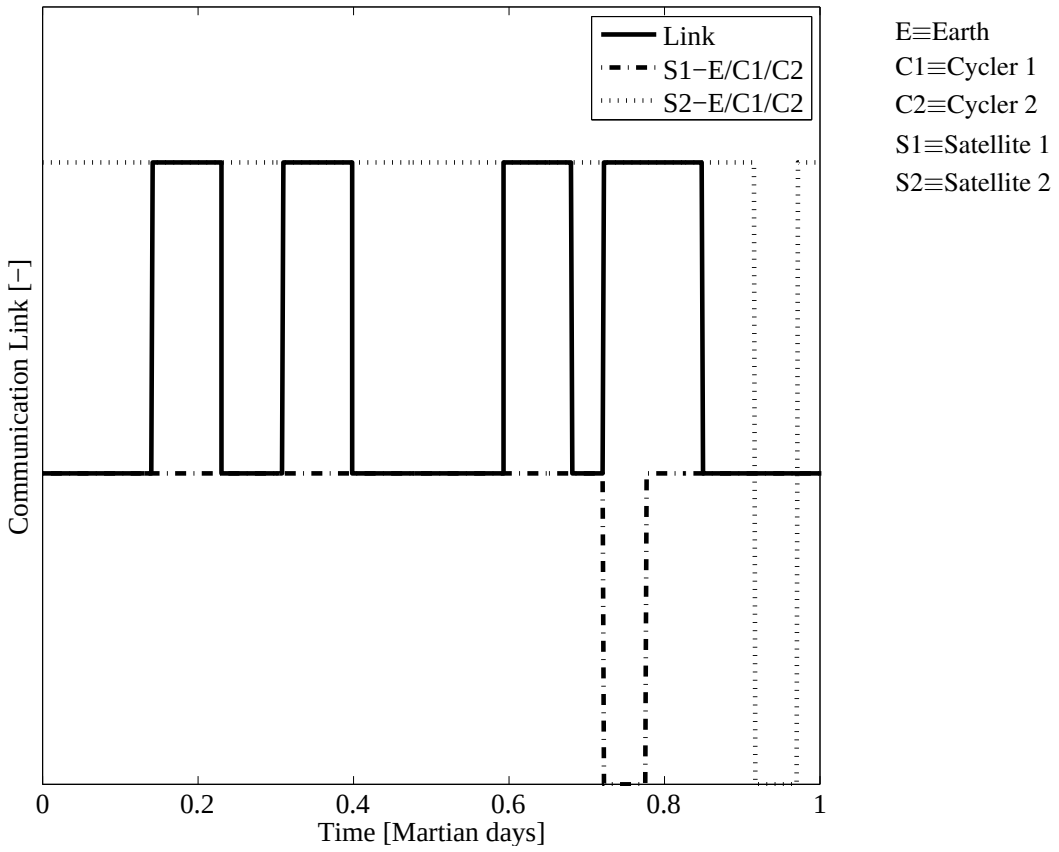

Figure 4.10: Availability of Communication Links from Satellites, Areostationary Orbit

The communication link between a satellite and Earth will be available unless the Earth, the satellite and Mars are aligned.

In Fig. 4.10 it is observed that, for all times, there is at least one satellite that can communicate with the Earth: when Satellite 2 cannot communicate with Earth (gap in the dotted line), Satellite 1 can (no gaps in the dash-dotted line at that time), and vice versa. This is achieved by means of the angular separation between the satellites.

The solid line represents which satellite is used to communicate with the Earth over time: this sequence is determined by the availability of the communication links between Phobos and Mars, and between the satellites and Phobos.

Figure 4.11 is a representation of the availability of the communication link between the satellites and Phobos with the colony on Mars, during one sol. The satellites orbit around Mars at the same angular velocity than the colony on Mars spins around Mars itself (by the definition of a stationary orbit); therefore, the satellites and the colony on Mars will always be able to communicate with each other. Phobos, however, orbits around Mars faster than the colony on Mars spins around Mars, and so Phobos will only be visible from the colony on Mars for about 1/3 of the time, with a period of about half a sol:

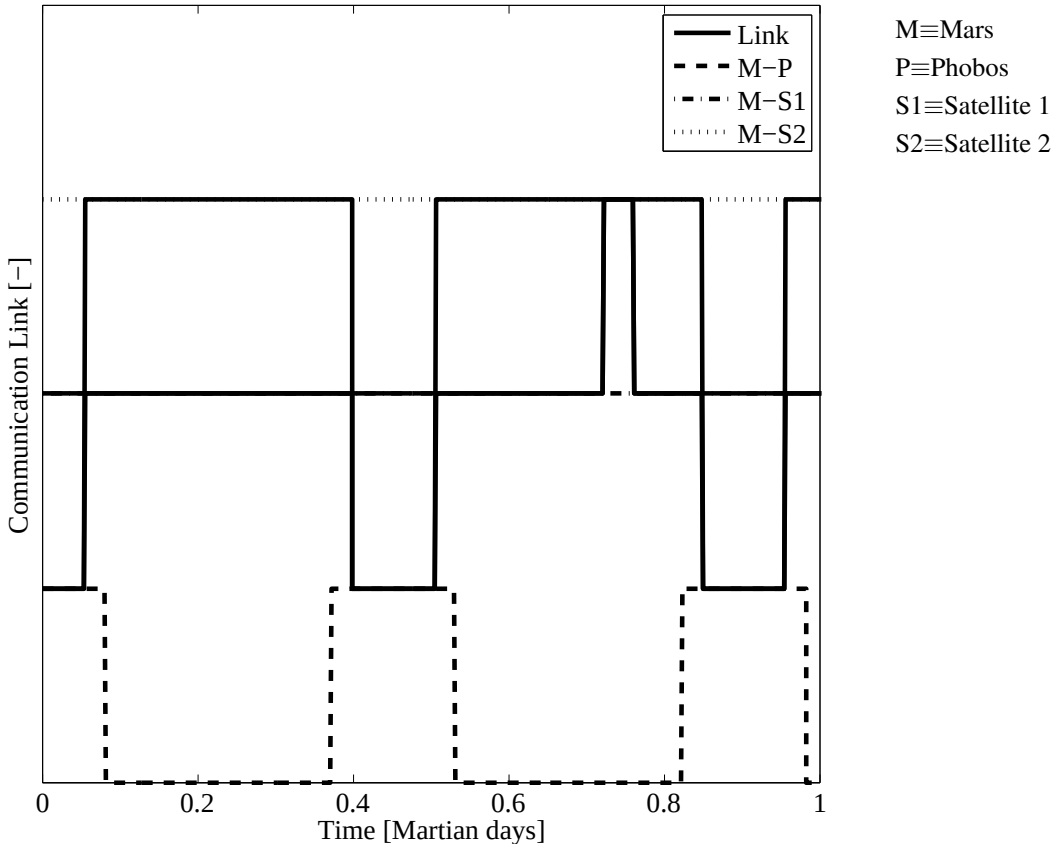

Figure 4.11: Availability of Communication Links from Mars, Areostationary Orbit

The solid line represents the communication sequence followed by the colony on Mars: the colony on Mars will always commmunicate with at least one of the satellites, so that information can be transmitted to Earth. If direct communication with Phobos is available, Mars will communicate directly with Phobos and with the satellite the communicates with Earth. The colony on Mars will communicate with both satellites at the same time when the signal needs to be relayed to Phobos (when Phobos is not visible from the colony on Mars), as one satellite will relay the signal to Phobos and the other satellite will communicate with Earth. If Phobos is not visible, the colony on Mars will communicate with one satellite to relay the signal to Phobos; if the other satellite cannot communicate with Earth at that particular time, the same satellite that relays the signal to Phobos will also communicate with Earth.

Figure 4.12 is a representation of the availability of the communication link from Phobos to the satellites and the colony on Mars, during one sol. It is observed that Phobos can communicate with at least one of the satellites or with Mars at all times. In this way, continuous communication between the colony on Phobos and the colony on Mars is possible:

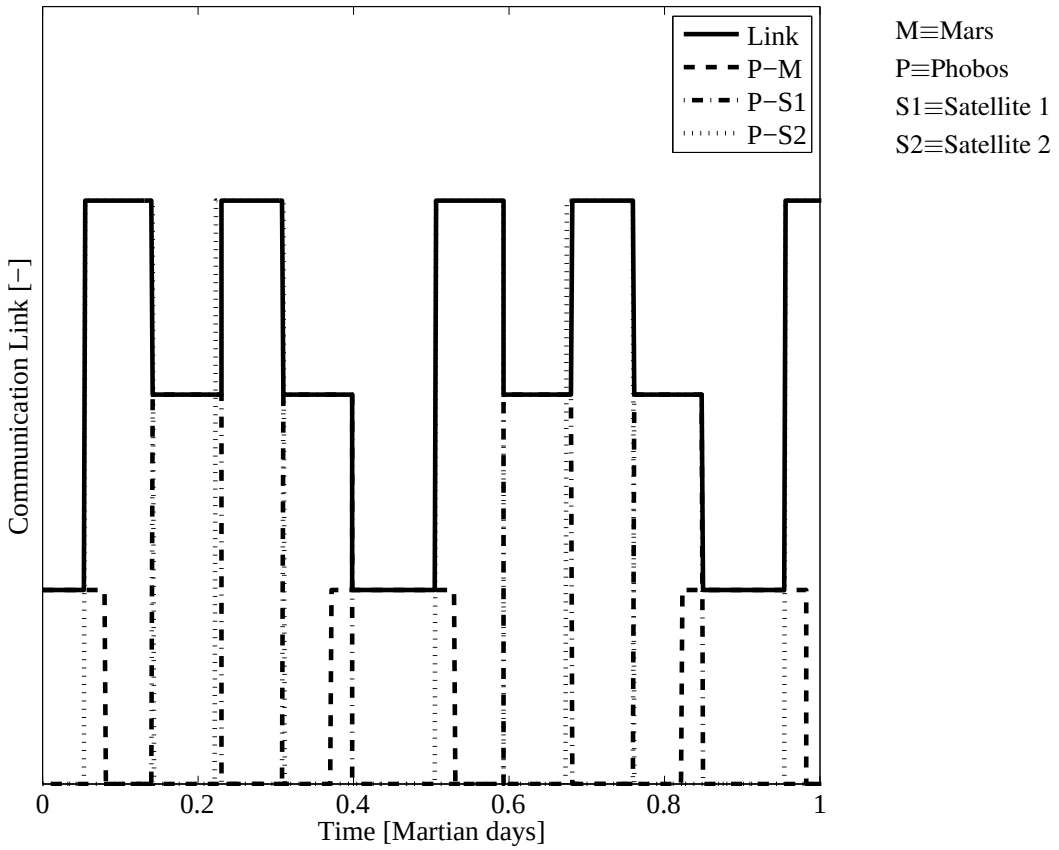

Figure 4.12: Availability of Communication Links from Phobos, Areostationary Orbit

The solid line represents the communication sequence followed by Phobos: Phobos will directly communicate with Mars when possible (if direct Mars-Phobos communication link is available–dashed line). If direct communication between Phobos and Mars is not available, Phobos will communicate only with one of the satellites and this satellite will relay the signal to the colony on Mars.

The main conclusion of this analysis is that continuous communication between the colonies on Phobos and Mars, and the Earth, can be provided with only two satellites around Mars, in an areostationary orbit.

4.5 Minimum Number of Antennas Required

Based on the visibility analyses performed in Sections 4.4.1 and 4.4.2, the minimum number of antennas required on Mars, Phobos, Satellite 1 and Satellite 2 can be calculated.

The criteria used to determined the number of antennas required is based on:

1. The number of communication links used at the same time: see, for instance, in Fig. 4.11, that the colony on Mars will communicate with the colony on Phobos and one of the communication satellites (at 0.5 Martian days), or with both satellites (at 0.2 Martian days), at the same time. It could then be concluded that a minimum number of at least two antennas will be required on the colony on Mars.
2. The communication sequence: using again the example in Fig. 4.11, at 0.4 Martian days, the colony on Mars will use two antennas to communication with both satellites at the same time; when direct communication with the colony on Phobos is recovered, the colony on Mars will stop communicating with Satellite 2 (communication is kept with Satellite 1) and start communicating with the colony on Phobos. As Satellite 2 and Phobos are at different orientations from the colony on Mars, the same antenna that was previously used to communicate with Satellite 2 cannot be used to communicate with the colony on Phobos, as an instantaneous–not possible–change of the antenna orientation would be required. Therefore, not only two but a minimum of three antennas will be required on the colony on Mars.

The same reasoning is followed for the number of antennas on the colony on Phobos, and the number of antennas on the satellites, for both of the proposed solutions for the communications satellite constellation around Mars.

4.5.1 Two Communication Satellites in Phobos' Orbit

Table 4.1 summarizes the minimum number of antennas required on Mars, Phobos, Satellite 1 and Satellite 2, for the communications satellite constellation in Phobos' orbit.

Table 4.1: Minimum Number of Antennas Required, Phobos' Orbit

Location	Number of Antennas	Type
Colony on Mars	2	Short-range antennas. Only one antenna is used at a time.
Colony on Phobos	3	Short-range antennas. Only two antennas are used at a time, during $\frac{1}{3}$ of the time.
Satellite 1/Satellite 2	3	Two short-range and one long-range antennas. The three antennas are used at the same time during 6-7 hours per Martian day.

4.5.2 Two Communication Satellites in an Areostationary Orbit

Table 4.2 summarizes the minimum number of antennas required on Mars, Phobos, Satellite 1 and Satellite 2, for the communications satellite constellation in an areostationary orbit:

Table 4.2: Minimum Number of Antennas Required, Areostationary Orbit Configuration

	Number of Antennas	Type
Colony on Mars	3	Short-range antennas. Only two antennas are used at a time.
Colony on Phobos	2	Short-range antennas. Only one antenna is used at a time.
Satellite 1/Satellite 2	3	Two short-range and one long-range antennas. The three antennas are used at the same time, during 1-2 hours per Martian day.

4.6 Limitations

Both solutions already proposed show limitations in terms of the maximum latitude at which the colony on Mars can be located, above which the solutions proposed are not valid.

The two solutions also show limitations in terms of the elevation angle above the horizon, ε, at which the communication satellites or Phobos are observed from the colony on Mars along time. The elevation angle will determine the quality of the communication link, as the larger the elevation angle, the lower the atmospheric attenuation on the signal.

4.6.1 Two Communication Satellites in Phobos' Orbit

Based on the geometry of the problem (see Fig. 4.2), the minimum elevation angle at which the colony on Mars communicates with the colony on Phobos or the communication satellites occurs under the geometric configuration represented in Fig. 4.13:

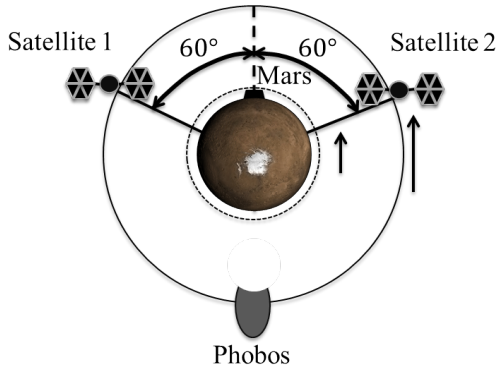

Figure 4.13: Minimum Elevation Angle Configuration

At such an instant, and in this particular case, communication between the colony on Mars and Satellite 1 will be lost, and communication between Satellite 2 and the colony on Mars will be enabled.

In order for continuous coverage to be provided by the given satellite constellation, and continuing with the particular case represented in Fig. 4.13, the colony on Mars should be able to communicate with Satellite 2 when the longitude difference, $\Delta\phi$, between Satellite 2 and the colony on Mars is 60°.

The maximum $\Delta\phi$ the colony on Mars is able to communicate with is dependent on the latitude of the colony, and it is reduced as the colony is located closer to the poles. Continuous communication can be provided with the given satellite constellation when the maximum $\Delta\phi$ is larger than the worst case scenario $\Delta\phi_{cr} = 60°$.

Under the assumption that communication is possible if visible 5° above the horizon (assumption (5) in Sec. 4.2), Fig. 4.14 represents the $\Delta\phi$ with which the colony on Mars can communicate (solid line) as a function of the latitude at which the colony is located, λ:

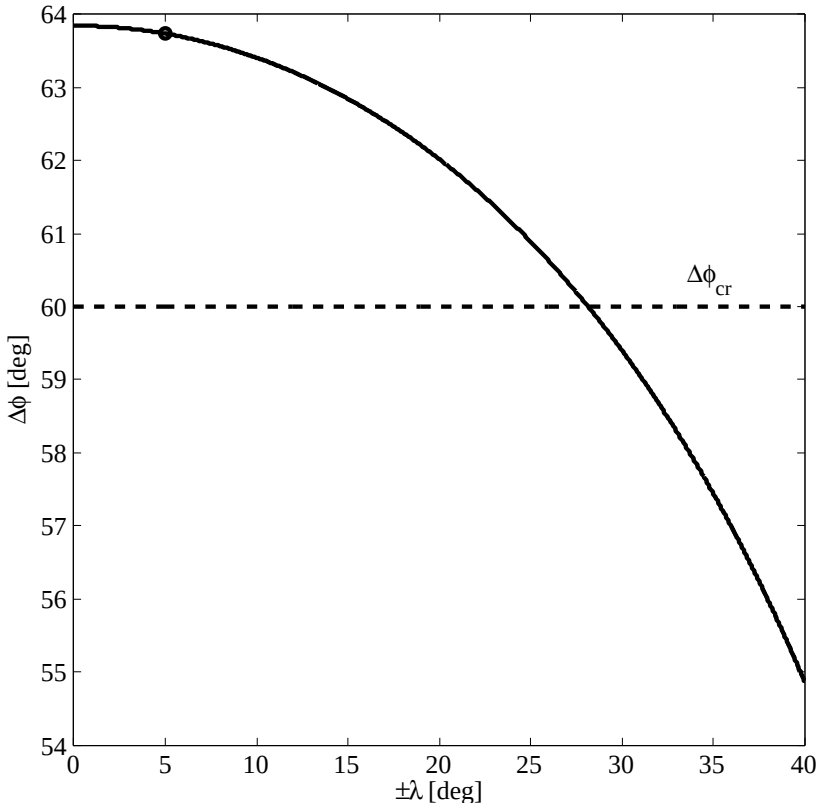

Figure 4.14: $\Delta\phi$ as a function of Latitude of the Colony

In Fig. 4.14, the black dot represents the maximum $\Delta\phi$ corresponding to the latitude at which the colony is assumed to be: $\lambda = \pm 5°$ (assumption (1) in Sec. 4.2).

For latitudes of the colony larger than $\lambda = \pm 28.2°$, the maximum $\Delta\phi$ is smaller than the required $\Delta\phi_{cr}$, and so, continuous communication cannot be achieved with the given satellite constellation if the colony is located above that latitude. The given satellite constellation is, however, a valid solution if the colony is located at any latitude below $\lambda = \pm 28.2°$.

In a similar way, the minimum elevation angle at which the colony on Mars will communicate with the satellites or with the colony on Phobos will occur under the geometric configuration shown in Fig. 4.13, and it is also

a function of the latitude of the colony.

Fig. 4.15 is a representation of the minimum elevation, ε, at which the colony on Mars will have to communicate with the satellites or the colony on Phobos (solid line), as a function of the latitude at which the colony is located, λ:

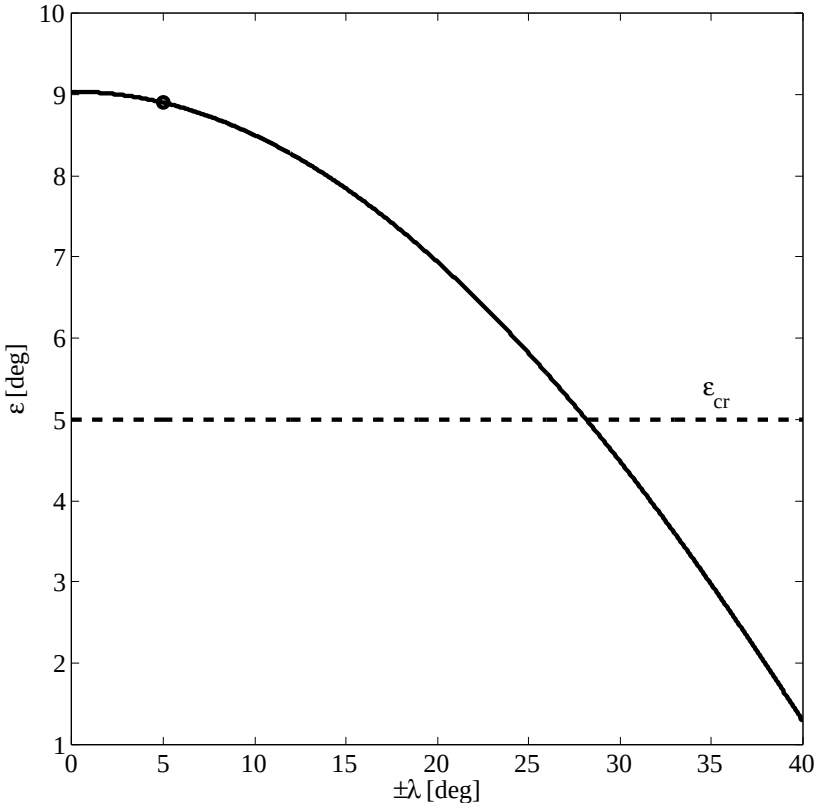

Figure 4.15: Minimum Elevation as a function of Latitude of the Colony

In Fig. 4.15, the black dot represents the minimum ε corresponding to the latitude at which the colony is assumed to be: $\lambda = \pm 5^\circ$ (assumption (1) in Sec. 4.2).

For latitudes of the colony larger than $\lambda = \pm 28.2^\circ$, the minimum ε is smaller than the required $\varepsilon_{cr} = 5^\circ$, and so, continuous communication cannot be achieved with the given satellite constellation if the colony is located beyond that latitude (as already concluded from Fig. 4.14).

It is worth noticing in Fig. 4.15 that ε is smaller than 10° even for a colony at 0° Latitude. Elevation angles for communication below 15° are often undesirable and inefficient due to large atmospheric attenuations. Therefore, the solution here provided is valid if the colony is located at any latitude below $\lambda = \pm 28.2^\circ$, as continuous coverage is provided, but it would imply high power requirements (or large antenna sizes) due to severe atmospheric attenuation.

4.6.2 Two Communication Satellites in an Areostationary Orbit

The geometry of the given configuration (see Fig. 4.4) is dependent on the latitude of the colony, as stated in Sec. 4.3.2. The angular separation between the two communication satellites, α, should lie within a particular range of angles: the range of values of α within which the satellites should be located to provide continuous communication

is dependent on the latitude of the colony; at the same time, this range is reduced the larger the latitude of the colony, up to a latitude at which the range of α is zero, and above which the solution is not valid as continuous communication could not be provided.

Under the given satellite constellation, there are three geometric configurations along a full orbit of Phobos around Mars for which communication between the colony on Phobos and one of the satellites, or the colony on Mars, becomes critical for continuous coverage. These three critical configurations define the range of angular separation between the communication satellites, α_{min} and α_{max}, within which continuous communication is provided.

The maximum angular separation between the communication satellites, α_{max} is determined by the geometric configuration shown in Fig. 4.16:

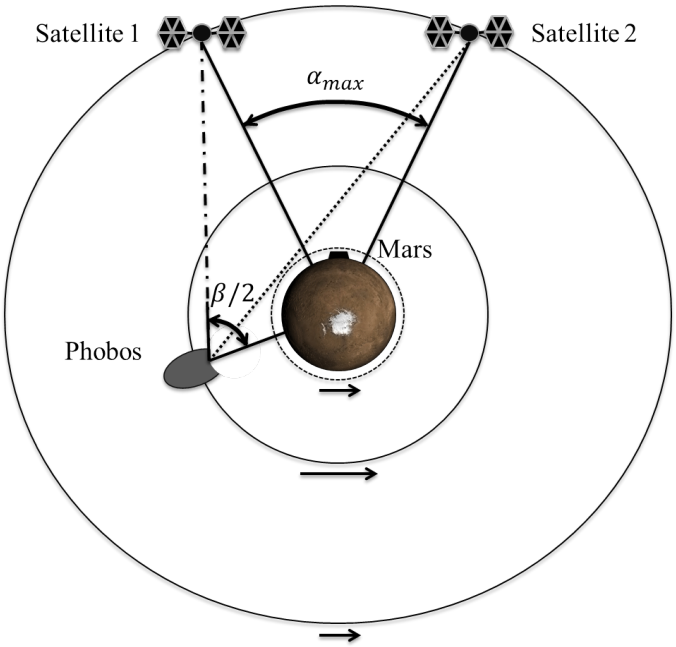

Figure 4.16: Maximum Angular Separation Configuration

Figure 4.16 illustrates the particular moment when the colony on Phobos is communicating with Satellite 2, but as Satellite 2 hides behind Mars, communication with Satellite 1 should be enabled (limited by the maximum angular visibility β from Phobos, assumption (2) in Sec. 4.2). This particular geometric configuration determines $\alpha_{max} = 70.5$, which is independent on the latitude of the colony.

The lower limit for the angular separation between the satellites, α_{min}, is defined as the maximum between $\alpha_{min,1}$ and $\alpha_{min,2}$, which are determined by the geometric configurations shown in Figures 4.17 and 4.18, respectively.

Figure 4.17 shows the geometric configuration from which $\alpha_{min,1}$ is determined:

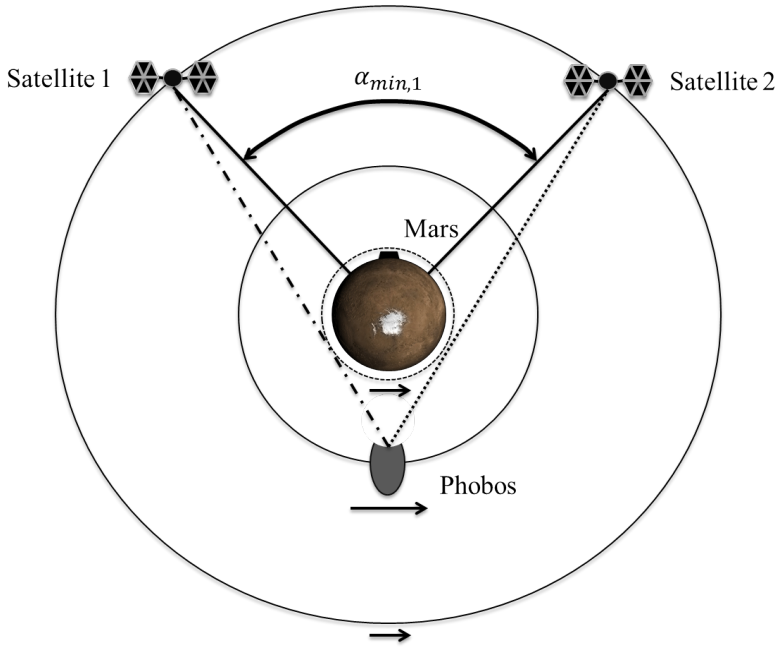

Figure 4.17: Minimum Angular Separation 1 Configuration

Figure 4.17 illustrates the particular moment when the colony on Phobos is communicating with Satellite 1, but as Satellite 1 hides behind Mars, communication with Satellite 2 should be enabled (Satellite 2 should become visible after being hidden behind Mars). This particular geometric configuration determines $\alpha_{min,1} = 63.9$, which is independent on the latitude of the colony.

Figure 4.18 shows the geometric configuration from which $\alpha_{min,2}$ is determined:

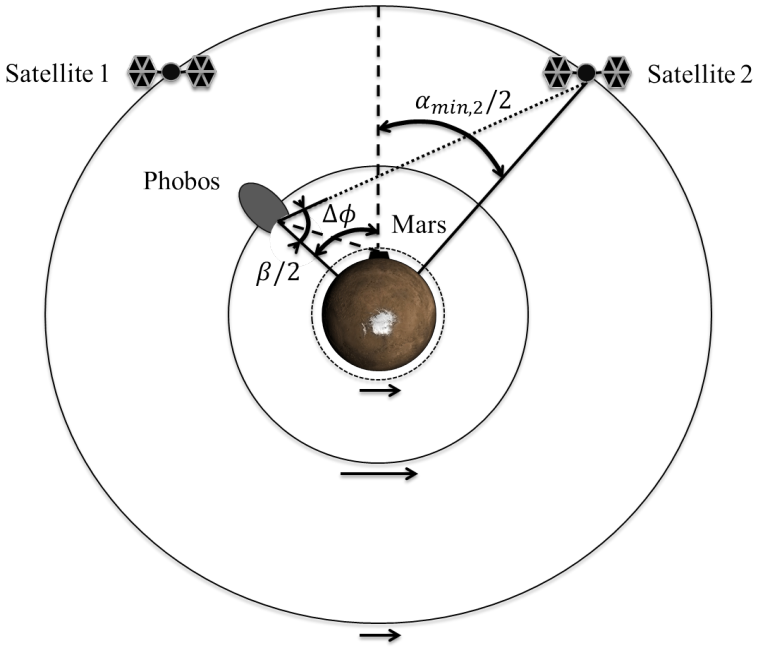

Figure 4.18: Minimum Angular Separation 2 Configuration

Figure 4.18 illustrates the particular moment when the colony on Phobos is communicating directly with the colony on Mars, but as Phobos orbits around Mars, the longitude difference, $\Delta\phi$, between Phobos and the colony on Mars reaches the maximum $\Delta\phi$ the colony on Mars can communicate with (which is a function of the latitude of the colony and the minimum elevation angle, ε_{cr}, below which the colony on Mars cannot communicate due to severe atmospheric attenuation). As direct communication with the colony on Mars is lost, communication between the colony on Phobos and Satellite 2 should be enabled (limited by the maximum angular visibility β from Phobos, assumption (2) in Sec. 4.2). This particular geometric configuration determines $\alpha_{min,2}$, which is then dependent on the latitude of the colony, λ, and ε_{cr}.

Figure 4.19 is a representation of the limits for the angular separation between the communication satellites within which continuous communication is provided with the proposed solution. For latitudes above the latitude at which $\alpha_{min,2}$ becomes larger than α_{max}, continuous coverage cannot be provided with this particular satellite constellation:

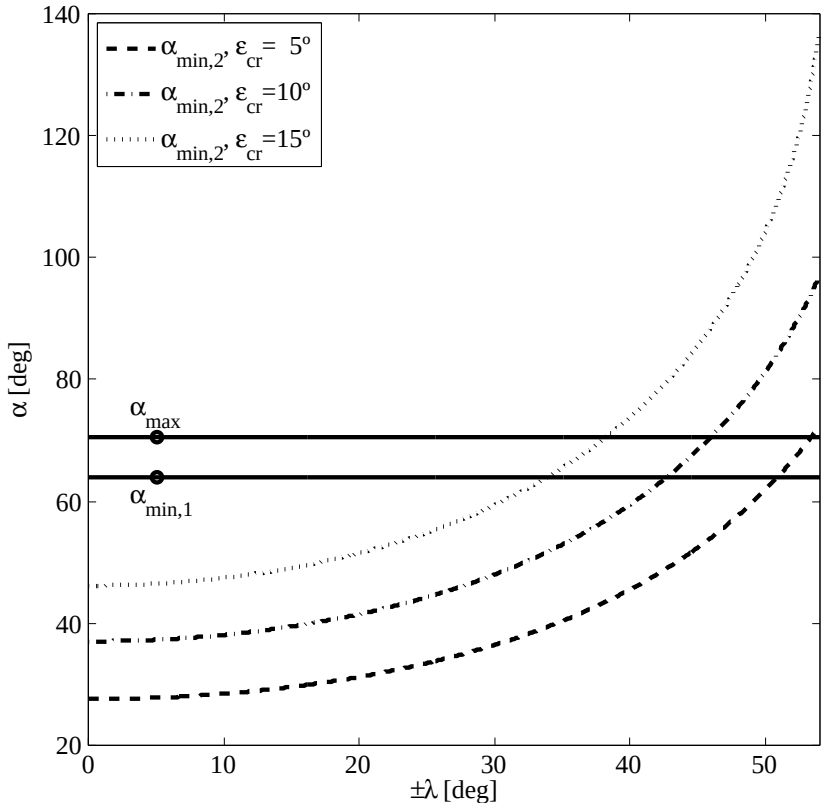

Figure 4.19: Limits for Angular Separation between the Satellites as a function of Latitude of the Colony

The solid lines represent α_{max} and $\alpha_{min,1}$, which, as already mentioned, are independent on the latitude of the colony. The lower limit $\alpha_{min,2}$ determined based on the configuration shown in Fig. 4.18 is represented as a function of the latitude of the colony for three values of ε_{cr}. For the assumed latitude of the colony $\lambda = \pm 5^{\circ}$, the lower and upper limits of α within which the communication satellites should be placed to provide continuous coverage are represented with black dots. At $\lambda = \pm 5^{\circ}$, $\alpha_{min,1} > \alpha_{min,2}$ so that the lower limit of α is determined by $\alpha_{min,1}$.

For $\varepsilon_{cr} = 5^{\circ}$ and latitudes of the colony above 50.9°, the lower limit of α is determined by $\alpha_{min,2}$; and for latitudes of the colony above 53.4°, continuous communication cannot be provided as $\alpha_{min,2} > \alpha_{max}$.

With two satellites in an areostationary orbit, unlike the other solution proposed of two satellites in Phobos' orbit, continuous communication can also be provided if $\varepsilon_{cr} = 15^{\circ}$ for latitudes of the colony below 38.2°, which is highly beneficial in terms of atmospheric attenuation.

4.7 Comparison of the Proposed Solutions

Both solutions for the problem under study (two satellites in Phobos' orbit and two areostationary satellites) are now compared based on the number of antennas required on Mars, Phobos and the satellites, the amount of time these antennas are used (Sec. 4.5), the limitations that these two solutions show in terms of the maximum latitude

at which these solutions are valid, and the quality of the communication link regarding atmospheric attenuation (Sec. 4.6):

1. Two satellites in Phobos' orbit are more convenient in terms of number of antennas used on Mars, as only one antenna is used at a time (instead of two), and only two antennas in total are required (instead of 3).
2. Two areostationary satellites are more convenient in terms of number of antennas used on Phobos, as only one antenna is used at a time (instead of two for $\frac{1}{3}$ of the time) and only two antennas in total are required (instead of 3).
3. Two areostationary satellites are more convenient in terms of number of antennas used on the satellites, as the amount of time the three antennas on the satellites are used at a time is considerably shorter (1-2 hours per sol instead of 6-7 hours per sol).
4. Two areostationary satellites are more convenient in terms of the maximum latitude at which the colony on Mars can be located ($\lambda_{max} = 53.4°$ instead of $\lambda_{max} = 28.2°$, for $\varepsilon_{cr} = 5°$).
5. Two areostationary satellites are more convenient in terms of the elevation angle at which the colony on Mars communicates with the colony on Phobos and with the communication satellites (valid for $\varepsilon_{cr} = [5°, 10°, 15°]$ instead of only $\varepsilon_{cr} = 5°$).

Two areostationary satellites is chosen to be the most convenient solution for the Mars-centered communications satellite constellation as the power and energy consumption on Phobos and the satellites is smaller due to the fewer number of antennas required and the amount of time these antennas are used.

Two satellites in Phobos' orbit are in fact more convenient in terms of the numbers of antennas required on Mars, however, the quality of the communication link in terms of atmospheric attenuation is lower, which would need to be compensated by a larger power and energy consumption, and the range of latitudes for which two satellites in Phobos' orbit are a valid solution is smaller.

It is also reasonable to assume that the availability of power and energy on Mars will be considerably larger than on Phobos and on the satellites; and therefore, even if the number of antennas required on Mars is higher, two areostationary satellites still hold as the most convenient solution among the two proposed solution.

5 Link Budget Analysis

The procedure followed to design and size each of the communication links necessary to provide continuous communication between Earth and the colonies on Mars and Phobos is now described in detail. The design and sizing of a communication architecture consists in specifying the transmitter and receive antenna diameters of a transmitted signal, the input power at the transmitter, and the frequency of the signal, for each of the communication links of that communication architecture.

5.1 Main Assumptions

The main assumptions for the current analysis are the same as the ones described in Sec. 4.2, except for assumption (5) in Sec. 4.2 that is modified to:

5. Communication between the colony on Mars and the satellites, or Phobos, is not possible unless they are visible above a minimum elevation angle above the horizon $\varepsilon_{cr} = 15^\circ$ (equivalent maximum visibility angle β of 150° for colony on Mars).

Recall that, according to Fig. 4.19, two areostationary satellites can provide continuous communication even if the minimum elevation angle is $\varepsilon_{cr} = 15^\circ$ for a latitude of the colony on Mars $\lambda = \pm 5^\circ$, so that:

6. The communications satellite constellation around Mars is composed of two areostationary satellites separated by an angular distance $\alpha = 65^\circ$ (see Sec. 4.3.2).
7. Most demanding configuration is considered while evaluating the link requirements, which means:
   (a) When communicating from or to the ground stations on Earth, or to the colony on Mars, the signal travels through the atmosphere at an elevation angle $\varepsilon_{cr} = 15^\circ$ above the horizon; except for the communication link between the colony on Mars and the areostationary satellites, as the orientation of the areostationary satellites with respect to the colony on Mars is known and kept the same for all times: $\varepsilon = 50^\circ$.
   (b) Propagation path length is the maximum propagation path length for each of the communication links.
8. The antennas on the colony on Mars, the antennas on the colony on Phobos and two of the antennas on the areostationary satellites are the same size (except for the antennas providing the communication link from the areostationary satellites to Earth or the cyclers), for simplcity in the manufacturing process.
9. The antennas on the cyclers and on the communication satellites (the antennas that provide the communication link from the areostationary satellites to Earth and to the cyclers) are the same size.
10. The communication architecture transmits an HDTV signal (to account for a very demanding case) from the colonies on Phobos and Mars to Earth.

And as a consequence of assumptions (8, 9), the power requirements for the antennas will be different depending on the link that these antennas provide along time (e.g. antennas on the areostationary satellites will provide direct link from Mars to Earth at times, and link to the cyclers at other times), and always equal or smaller than the maximum power requirements computed in this study.

5.2 Communication Links

The communication links that need to be designed and sized are illustrated and enumerated below in Fig. 5.1:

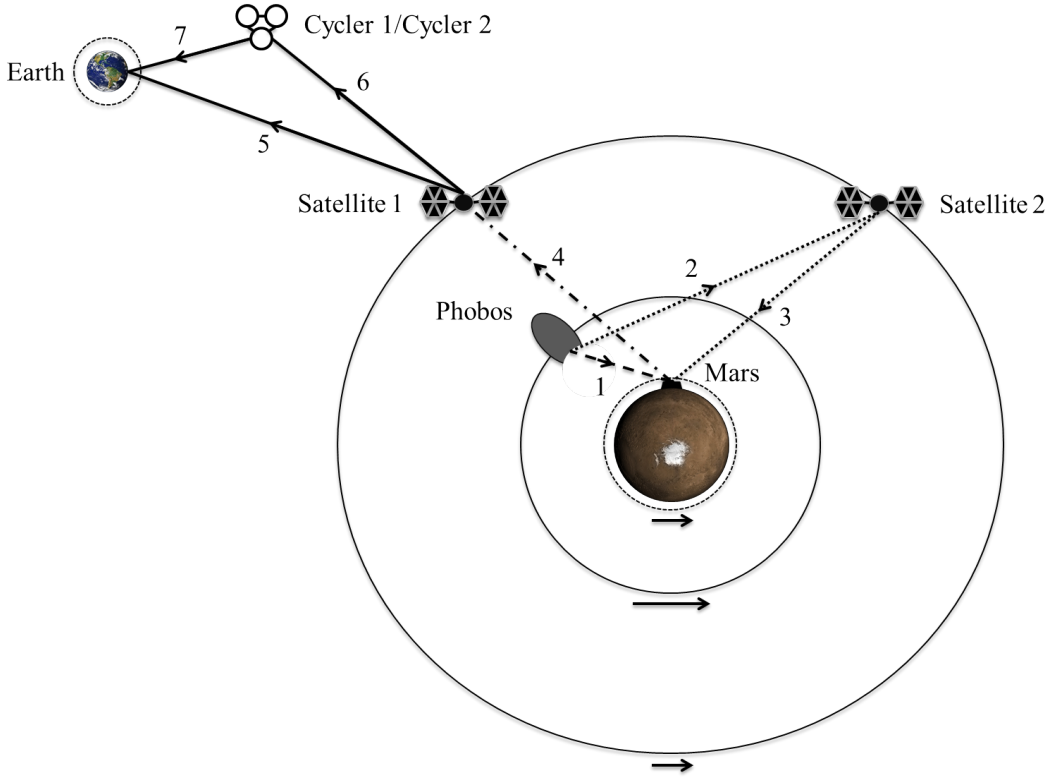

Figure 5.1: Communication Links

These communication links are named and described below (notice that the enumeration below corresponds to the numbers in Fig. 5.1):

1. Link Phobos-Mars represents the downlink from the colony on Phobos to the colony on Mars when the direct Phobos-Mars link is available (interaction with Mars' atmosphere).
2. Link Phobos-Satellite represents the communication link between the colony on Phobos and one of the communication satellites (in this case, Satellite 2) used to relay the signal from the colony on Phobos to the colony on Mars when the direct Phobos-Mars link is not available.
3. Link Mars-Satellite (Downlink) represents the link from one of the communication satellites (in this case, Satellite 2) to the colony on Mars used to deliver the signal from the colony on Phobos to the colony on Mars when the direct Phobos-Mars link is not available (interaction with Mars' atmosphere).
4. Link Mars-Satellite (Uplink) represents the link from the colony on Mars to one of the communication satellites (in this case, Satellite 1) used to send both, the signal from the colony on Phobos and from the colony on Mars, to Earth (interaction with Mars' atmosphere).
5. Link Satellite-Earth represents the direct downlink from Mars to Earth used to send the signal from the surroundings of Mars to the ground stations on Earth when the cyclers are not used as communication relays (interaction with Earth's atmosphere).

6. Link Satellite-Cycler represents the communication link necessary to transfer the signal from the surroundings of Mars to one of the cyclers during Earth-Mars solar conjunction.

7. Link Cycler-Earth represents the downlink from one of the cyclers to the ground stations on Earth used to transfer the signal coming from Mars to Earth during Earth-Mars solar conjunction (interaction with Earth's atmosphere).

5.3 Maximum Propagation Path Length

The maximum propagation path lengths for the communication links that need to be designed and sized are summarized in Table 5.1 below:

Table 5.1: Maximum Propagation Path Lengths

Communication Link	Propagation Path Length [km]	Comments
Phobos-Mars	7904	Interaction with Mars' atmosphere at $\varepsilon = 15°$.
Phobos-Satellite	28780	
Mars-Satellite (Downlink)	17658	Interaction with Mars' atmosphere at $\varepsilon = 50°$.
Mars-Satellite (Uplink)	17658	Interaction with Mars' atmosphere at $\varepsilon = 50°$.
Satellite-Earth	374124880	Interaction with Earth's atmosphere at $\varepsilon = 15°$.
Satellite-Cycler	404054870	
Cycler-Earth	59859981	Interaction with Earth's atmosphere at $\varepsilon = 15°$.

The maximum propagation path lengths for the links Cycler-Earth, Satellite-Cycler and Satellite-Earth were previously mentioned in Table 3.1. The geometric configuration that yields maximum propagation path length for the link Phobos-Satellite was previously represented in Fig. 4.17. Maximum propagation path length for the links Phobos-Mars and Mars-Satellite (Uplink and Downlink) are computed with Fig. 4.6 as reference.

5.4 Link Equation

The criteria followed to design and size the communication links of the mission consists in determining the energy carried by a received signal after being attenuated by several factors (such as the interaction with the atmosphere or noise sources) that weaken the signal; if the energy received exceeds a certain threshold, the signal can be read and reproduced at the destination.

The link equation used to size the digital data link [34] is:

$$\frac{E_b}{N_0} = \frac{PL_l G_t L_s L_a G_r}{kT_s R}, \tag{5.1}$$

where E_b/N_0 is the ratio of received energy-per-bit to noise-density (or noise spectral density), which defines the capacity of a sent bit to be reproduced correctly when received. The parameter E_b/N_0 should remain above a specific value (minimum E_b/N_0 will be specified later in this section) when transmitting a signal in order for the communication link to be properly sized.

The transmitter power, P, is the input power at the particular antenna where the signal is generated.

The transmitter-to-antenna line loss, L_l, is the inherent loss produced in the onboard systems. Due to the unavailability of analytical models for L_l, the transmitter line loss is estimated as directly proportional to the transmitter power:

$$L_l = 2.3 \cdot 10^{-2} \cdot P, \tag{5.2}$$

where L_l is in dB and P is in dBm (a number expressed in decibels is $10 \cdot log_{10}$ of that number; if the number has units, the units are attached to the dB notation: $1000\ W$ is $30\ dBW$). The relationship between L_l and P is estimated based on the proportionality between L_l and P in the link performance of the Galileo [35], Cassini Orbiter/Huygens [36], Dawn [37], Juno [38], and Odyssey [39] missions.

The transmit antenna peak gain, G_t, and the receive antenna peak gain, G_r, are computed as:

$$G = \frac{\pi^2 D^2 \eta}{\lambda^2}, \tag{5.3}$$

where D is the corresponding antenna diameter (D_t for the transmitter antenna diameter and D_r for the receive antenna diameter), η is the corresponding antenna efficiency, and $\lambda = c/f$ is the wavelength of the transmitted signal ($c = 3 \cdot 10^8\ m/s$ is the speed of light and f is the frequency of the signal, which is specified later in Sec. 5.6.1). Again, due to the unavailability of information in this matter, the efficiency of all the antennas on the cyclers, communication satellites, colonies on Phobos and Mars is estimated as $\eta = 0.59$ based on [35–39]. In the same manner, the efficiency of the ground station antennas is estimated as $\eta = 0.70$.

If the receive antenna is not exactly located at the center of the transmitter antenna beam, or vice versa, the gain is reduced from its peak value (Eq. 5.3). The loss caused by the pointing offset of the signal from the beam center is called pointing loss, L_θ, which is computed as:

$$L_\theta = -12 \left(e/\theta\right)^2, \tag{5.4}$$

where L_θ is in dB, e is the pointing error, and $\theta = 21/\left(f_{GHz} D\right)$ is the antenna half-power beamwidth (f_{GHz} is the frequency of the signal in GHz, θ is in degrees). Due to the unavailability of information in this matter, the pointing error is estimated as $e = 0.05°$ for all the antennas on the cyclers, communication satellites, colonies on Phobos and Mars (based on [35–39] and the Mars Exploration Rover mission [40]), and $e = 0.03°$ for the ground station antennas on Earth (based on [40] as well).

The radiated power (P) reduced by the line loss (L_l), the transmitter antenna pointing loss ($L_{\theta,t}$), and increased by the transmitter antenna gain (G_t) is defined as the effective isotropic radiated power (EIRP).

The space loss, L_s, is the attenuation of the signal due to the propagation path that this signal travels through space. Equation 5.5 relates the space loss to the frequency of the signal and the propagation path length, S, which should be replaced by the maximum propagation path length of each link (see Sec. 5.3):

$$L_s = \left(\frac{c}{4\pi S f}\right)^2. \tag{5.5}$$

The transmit path loss, L_a, is caused by the interaction with the atmosphere that the signal travels through (see Table 5.1). The transmit path loss is produced by two main factors: polarization loss, L_p, and atmospheric attenuation, τ.

Due to the unavailability of analytical models for L_p, the polarization loss is estimated as directly proportional to the receive antenna peak gain (based on [35–40]):

$$L_p = -6.5 \cdot 10^{-3} \cdot G_r, \tag{5.6}$$

where L_p and G_r are in dB.

The atmospheric attenuation is due to the gaseous absortion of oxygen and water vapor. The atmospheric attenuation is dependent on the elevation angle above the horizon, ε, at which the signal travels through the atmosphere.

Figure 5.2 represents the zenith atmospheric attenuation, τ_{90°, as a function of the frequency of the signal for Earth's atmosphere [41]:

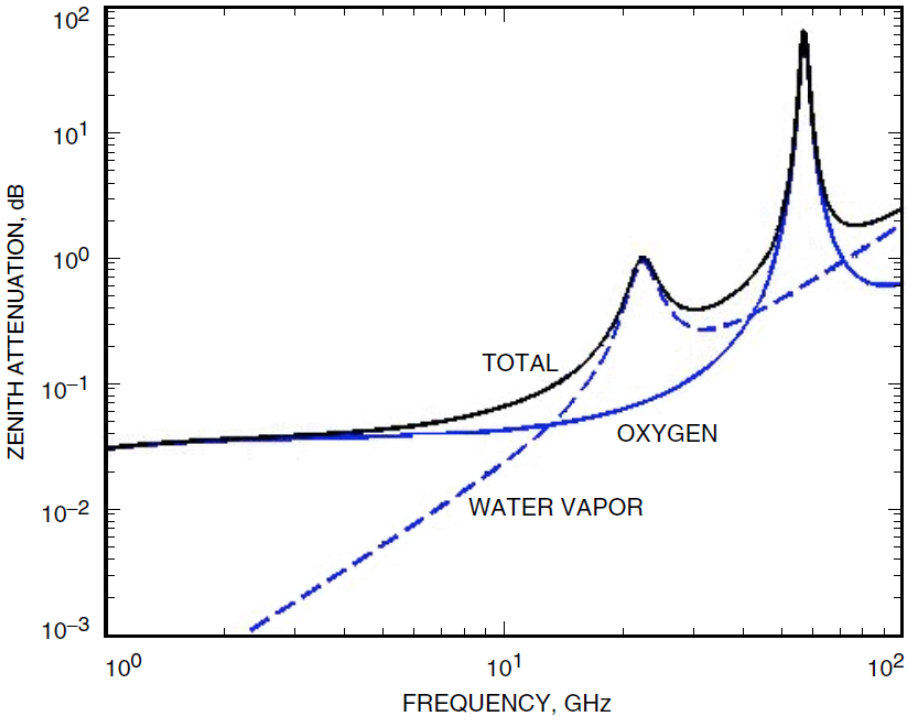

Figure 5.2: Zenith Atmospheric Attenuation, Earth's Atmosphere. Retrieved from [41]

The zenith atmospheric attenuation, τ_{90°, as a function of the frequency of the signal for Mars's atmosphere [42], in this case, is represented in Fig. 5.3 below:

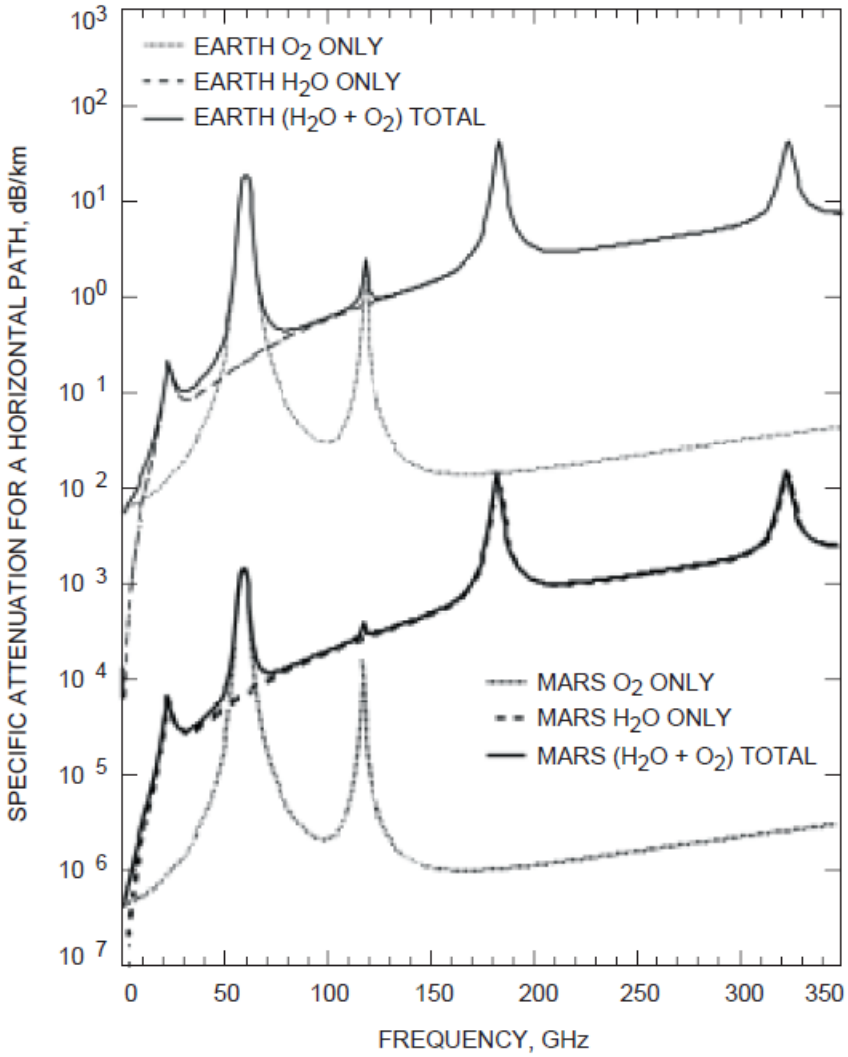

Figure 5.3: Zenith Atmospheric Attenuation, Mars's Atmosphere. Retrieved from [42]

Equation 5.7 is used to relate the zenith atmospheric attenuation, τ_{90°, to the attenuation at an elevation angle ε (τ_ε):

$$\tau_\varepsilon = \tau_{90^\circ}/sin(\varepsilon). \tag{5.7}$$

The radiated power increased by the transmitter and receive antenna gains, and reduced by the line loss, pointing loss of the transmitter and receive antennas, and by the polarization and atmospheric losses is defined as the total received power, P_t.

The system noise temperature, T_s or SNT, expresses the total noise produced in the system. In this study, three noise sources are considered: the antenna, the atmosphere and the cosmic background.

Due to the unavailability of analytical models, the downlink SNT due to the antenna is estimated to be 25 K if the signal travels through the Earth's atmosphere [34], and 4 K if the signal travels through Mars' atmosphere [42],

based on the frequency of the signal. The uplink SNT due to the antenna on Mars is estimated to be 193 K [42].

The SNT due to the atmosphere as a function of the frequency for Earth's atmosphere is represented in Fig. 5.4 below [41], for different elevation angles, ε:

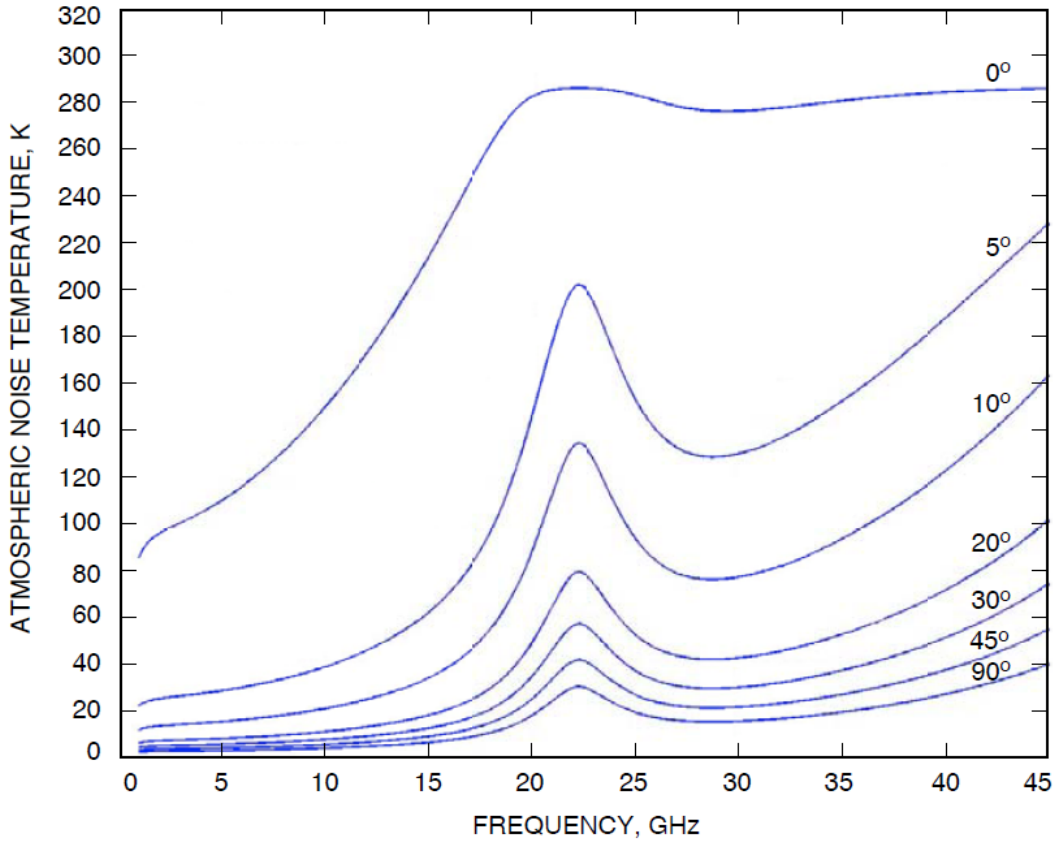

Figure 5.4: Atmospheric Noise Temperature, Earth's Atmosphere. Retrieved from [41]

For Mars's atmosphere, the SNT due to the atmosphere is 5 K in average [42]. In this study, the SNT due to Mars' atmosphere is estimated to be 10 K (accounting for some additional error margin) and independent on the elevation angle.

The SNT due to cosmic background is 2.7 K [34].

In Eq. 5.1, $k = 1.3806488 \cdot 10^{-23}\ m^2 \cdot kg \cdot s^{-2} \cdot K^{-1}$ is the Boltzmann's constant, which, multiplied by the system noise temperature, yields the noise spectral density, N_0:

$$N_0 = kT_s. \tag{5.8}$$

According to assumption (10) in Sec. 5.1, the communication architecture should transmit an HDTV signal from Mars to Earth. The data rate, R, required for good quality HDTV is standardized to be 12-14 Mbps [43]. For the problem under study, the data rate is specified to be $R = 14\ Mbps$.

The received energy per bit, E_b, can then be related to the received power as:

$$E_b = \frac{P_t}{R}. \tag{5.9}$$

The modulation, together with the bit error rate (BER), specifies the required E_b/N_0. The modulation is the process by which an input signal varies the amplitude, phase, frequency and/or polarization of a transmitted sine wave. The quadriphased phase shift keying (QPSK) is the phase modulation technique selected for the problem under study [44]. The BER is the probability for a data bit to be incorrectly received. The bit error rate should be smaller than 10^{-4} for good quality HDTV transmission [45]. In the problem under study, the bit error rate is specified to be $BER = 10^{-5}$ accounting for some additional error margin.

Figure 5.5 represents the BER as a function of the ratio E_b/N_0, for several modulation techniques [34]:

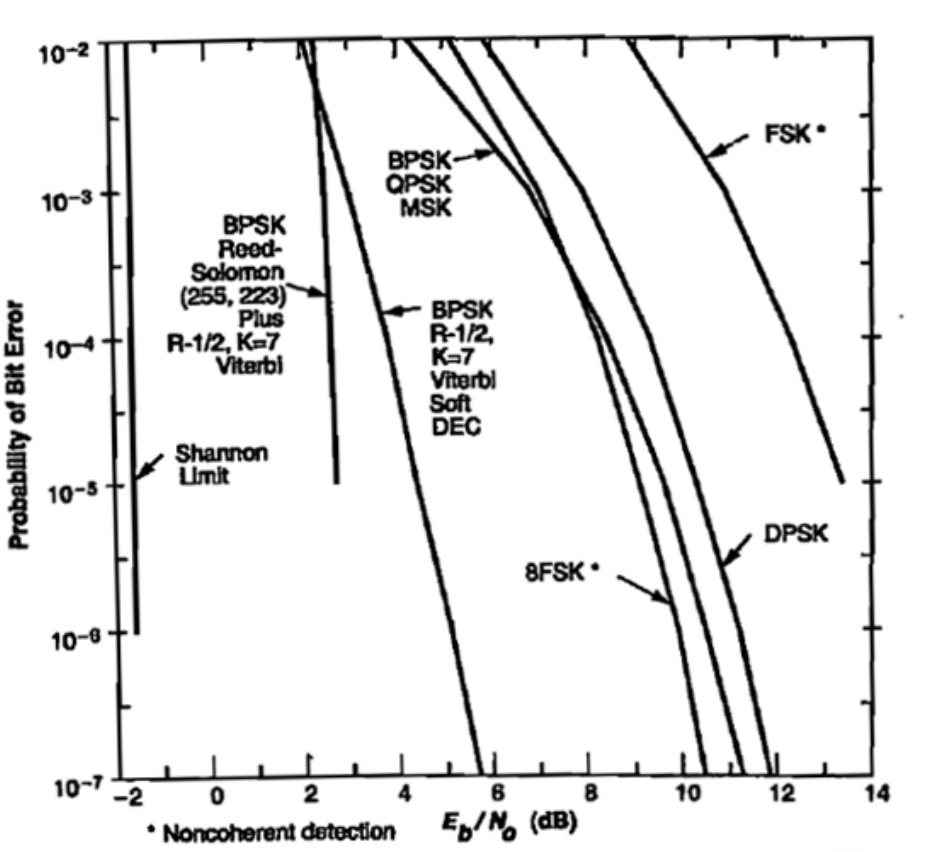

Figure 5.5: Bit Error Probability as a function of E_b/N_0. Retrieved from [34]

For the QPSK modulation technique and a BER of 10^{-5}, the minimum E_b/N_0 is 9.6 dB (see Fig. 5.5). Accounting for a 2 dB implementation loss, the required received energy-per-bit to noise-density ratio for the current mission is specified then to be $E_b/N_0 = 11.6\ dB$.

In addition, a required E_b/N_0 margin of 3 dB is considered between the available E_b/N_0 and the required E_b/N_0 to account for rain degradation.

5.5 Model Validation

The assumptions and procedure described to apply the link equation (Sec. 5.4) is now validated.

The link performance of the Juno X-band downlink (to Earth) at maximum range in 2016 is predicted under

the assumptions and following the procedure described in Sec. 5.4. The parameters summarized in Table 5.2 are used to apply the link equation (Eq. 5.1) in order to compare the Juno Telecommunications NASA results to the results obtained with the model here developed. It is worth to mention that the link budget analysis here performed is not as complex or detailed as the analysis developed by NASA due to the lack of open-source information and tools:

Table 5.2: Link Equation Parameters, Juno X-band dowlink at maximum range in 2016 [38]

Parameter	Value
Input Power, P [W]	25
Transmitter Antenna Diameter, D_t [m]	2.5
Frequency, f [GHz]	8.404135802
Propagation Path Length, S [km]	$9.6625 \cdot 10^8$
Ground Station (DSN) Antenna Diameter, D_r [m]	34
Data Rate, R [bps]	18000
Elevation Angle, ε [deg]	15

Table 5.3 compares the link performance of the Juno mission (NASA Results) to the link performance predicted under the assumptions of this study (Current Model), based on the parameters in Table 5.2:

Table 5.3: Link Performance Comparison, Juno X-band dowlink at maximum range in 2016

		Current Model	NASA Results [38]
	TRANSMITTER PARAMETERS		
1	Transmitter Power, P [dBm]	**43.98**	44.40
2	Line Loss, L_l [dB]	**-1.03**	-0.90
3	Transmitter Antenna Gain, G_t [dBi]	**44.48**	44.70
4	Transmitter Pointing Loss, $L_{\theta,t}$ [dB]	**0.03**	0.93
5	EIRP (1+2+3-4) [dBm]	**87.40**	87.37
	PATH PARAMETERS		
6	Space Loss, L_s [dB]	**-290.63**	-290.64
7	Atmospheric Attenuation, τ_ε [dB]	**-0.21**	-0.20
	RECEIVER PARAMETERS		
8	Receive Antenna Gain, G_r [dB]	**67.94**	68.26
9	Receiver Pointing Loss, $L_{\theta,r}$ [dB]	**-2.00**	-0.10
10	Polarization Loss, L_p [dB]	**-0.44**	-0.05
	TOTAL POWER SUMMARY		
11	Received Power (5+...+10), P_t [dBm]	**-137.95**	-135.40
12	SNT due to Antenna [K]	**25.00**	16.81
13	SNT due to Atmosphere [K]	**16.00**	12.78
14	SNT due to Cosmic Background [K]	**2.70**	2.60
15	SNT (12+13+14), T_s [K]	**43.70**	49.72
16	Noise Spectral Density [dBm/Hz]	**-182.20**	-181.63
17	Received P_t/N_0 [dB-Hz]	**44.25**	46.21
18	Data Rate, R [dB-Hz]	**42.55**	42.55
19	**Available E_b/N_0 (17-18) [dB]**	**1.70**	**2.60**

Recall that the current analysis is a simplified version of the analysis performed by NASA; in particular, a fewer number of contributions to the system noise temperature is considered, and additional losses are omitted between steps (17) and (19) in Table 5.3.

The current analysis does show certain inaccuracy. The inaccuracy of the current model is, however, taken care by conservative estimations of the antenna efficiencies (i.e. antenna gains), polarization loss, pointing errors (i.e pointing losses) and system noise temperature due to the antenna, atmosphere and cosmic background.

As a consequence, even if the model does not provide accurate results for every single parameter in the link budget analysis, the final, and most relevant, value for the available E_b/N_0 is accurately predicted. The model here developed provides a conservative estimation of the available E_b/N_0, and, therefore, a communication architecture developed with this model ensures proper performance of the communication architecture even under the worst expected conditions.

5.6 Link Design and Sizing

Once the model of this study to apply the link equation is validated, the link budget analysis is performed for the communication architecture of interest.

The process of link design and sizing is, in fact, iterative. The overall goal of the link design in this mission is to minimize the total mass of the communication architecture (i.e. to minimize the diameter of the antennas), with reasonable power requirements.

5.6.1 Frequency

Three main frequency bands are available for telecommunications: S-band (2-4 GHz), X-band (8-12 GHz) and Ka-band (26.5-40 GHz). The frequency of the signal has its main impact in the half-power beamwidth, antenna gain, space loss, atmospheric losses, and system noise temperature.

A higher frequency decreases the half-power beamwidth, which would increase the pointing loss for a given pointing error (increase in power requirement). A higher frequency increases the transmitter and receive antenna gains, which would decrease the power requirement. The space and atmospheric losses increase for higher frequency which would increase the power requirement as well. And finally, the system noise temperature is, typically, the largest for the Ka-band and the smallest for the X-band.

The X-band is concluded to be the most convenient frequency band for the problem under study due to its low system noise temperature, and higher transmitter and receive antenna gains than the S-band, and lower pointing, space and atmospheric losses than the Ka-band. The frequency of the signal is specified to be $f = 8.4\,GHz$ for all communication links, based on typical frequency values used in former NASA missions [35–40].

5.6.2 Antenna Diameter

Consequently to assumptions (8, 9) in Sec. 5.1, three antennas need to be sized: ground station antennas on Earth, antennas on cyclers (communications satellites will be equipped with one of these antennas as well), and antennas on Mars (communication satellites and colony on Phobos will be equipped with the same kind of antenna too).

For the ground station antennas on Earth, the Deep Space Network (DSN) is considered. The DSN is equipped with 26-m, 34-m and 70-m diameter antennas, which maximizes the receive antenna gain and therefore reduces the power requirement. However, due to its high operational costs and limited availability, the DSN is not chosen as ground stations for the current mission. Instead, fairly common and well-sized 10-m diameter antennas are chosen as ground station on Earth.

The communication links between the cyclers and Earth, between the cyclers and the communication satellites, and between the communication satellites and Earth are the most demanding communication links of the mission; therefore, a large diameter is convenient for the antennas that provide these communication links. With Galileo's high gain antenna (HGA) as a reference, the antennas on the cyclers are designed to be 4.8-m diameter antennas.

The communication links in the surroundings of Mars are not extremely demanding as the atmospheric attenuation due to Mars' atmosphere is, in fact, about three orders of magnitude smaller than the atmospheric attenuation due to Earth's atmosphere (see Fig. 5.3), and the propagation path lengths are also significantly smaller than for the other communication links of the mission. The antennas on Mars are designed to be 0.20-m diameter antennas.

5.6.3 Power Requirement

Once the antenna diameters and the frequency of the signal are specified, the transmitter input power should be sufficiently large for the available E_b/N_0 ratio to exceed, by a margin of 3 dB, the required $E_b/N_0 = 11.6\,dB$ ratio.

The power required for each of the communication links of the mission is specified in Sec. 5.7.

5.7 Link Performance

The link performance of each of the communication links of the mission is now analyzed.

Table 5.4 summarizes the parameters necessary to apply the link equation (Eq. 5.1), for each of the communication links: input power, P, transmitter antenna diameter, D_t, propagation path length, S, receive antenna diameter, D_r, and elevation angle, ε. The frequency for all the communication links is, as already specified, $f = 8.4\,GHz$ and the data rate is $R = 14\,Mbps$. Recall that a description of all the communication links of the mission is found in Sec. 5.2:

Table 5.4: Link Equation Parameters, Project Aldrin-Purdue

Communication Link	P [W]	D_t [m]	S [km]	D_r [m]	ε [deg]
Phobos-Mars	30	0.2	7904	0.2	15
Phobos-Satellite	65	0.2	28780	0.2	N/A
Mars-Satellite (Downlink)	155	0.2	17658	0.2	50
Mars-Satellite (Uplink)	2000	0.2	17658	0.2	50
Satellite-Earth	26100	4.8	374124880	10	15
Satellite-Cycler	49000	4.8	404054870	4.8	N/A
Cycler-Earth	615	4.8	59859981	10	15

$P \equiv$Input Power, $D_t \equiv$Transmitter Antenna Diameter, $S \equiv$Propagation Path Length, $D_r \equiv$Receive Antenna Diameter, $\varepsilon \equiv$Elevation Angle.

The power requirement on each communication satellite (a maximum total power requirement $P = 155\,W + 49000\,W = 49155\,W$ for telecommunications) is ensured by the Communications Team of Project Aldrin-Purdue by two 12-m diameter ATK MegaFlex solar panels; whereas the power requirement on each cycler (a maximum total power requirement $P = 615\,W$ for telecommunications) is ensured by two 28-m diameter ATK MegaFlex solar panels. The maximum total power requirement for telecommunications on the colony on Phobos is 65 W, and 2000 W on the colony on Mars.

The link equation for each of the communication links of the mission can now be applied, based on the information in Table 5.4. The link performance of all the communication links of the mission is found in Table 5.5 below:

Table 5.5: Link Performance, Project Aldrin-Purdue

		Communication Link						
		P-M	P-S	M-S (D.)	M-S (U.)	S-E	S-C	C-E
	TRANSMITTER PARAMETERS							
1	Transmitter Power, P [dBm]	44.47	48.13	51.90	63.01	74.17	76.90	57.89
2	Line Loss, L_l [dB]	-1.05	-1.13	-1.21	-1.47	-1.74	-1.80	-1.35
3	Transmitter Antenna Gain, G_t [dBi]	22.54	22.54	22.54	22.54	50.15	50.15	50.15
4	Transmitter Pointing Loss, $L_{\theta,t}$ [dB]	0.00	0.00	0.00	0.00	0.11	0.11	0.11
5	EIRP (1+2+3-4) [dBm]	66.26	69.54	73.23	84.08	122.47	125.14	106.57
	PATH PARAMETERS							
6	Space Loss, L_s [dB]	-188.88	-200.11	-195.89	-195.87	-282.39	-283.06	-266.47
7	Atmospheric Attenuation, τ_ε [dB]	0.00	0.00	0.00	0.00	-0.21	0.00	-0.21
	RECEIVER PARAMETERS							
8	Receive Antenna Gain, G_r [dB]	22.54	22.54	22.54	22.54	65.61	50.15	65.61
9	Receiver Pointing Loss, $L_{\theta,r}$ [dB]	0.00	0.00	0.00	0.00	-1.17	-0.11	-1.17
10	Polarization Loss, L_p [dB]	-0.15	-0.15	-0.15	-0.15	-0.43	-0.33	-0.43
	TOTAL POWER SUMMARY							
11	Received Power (5+...+10), P_t [dBm]	-100.23	-108.17	-100.26	-89.40	-96.13	-108.21	-96.10
12	SNT due to Antenna [K]	4.00	0.00	4.00	193.00	25.00	0.00	25.00
13	SNT due to Atmosphere [K]	10.00	0.00	10.00	10.00	16.00	0.00	16.00
14	SNT due to Cosmic Background [K]	2.70	2.70	2.70	2.70	2.70	2.70	2.70
15	SNT (12+13+14), T_s [K]	16.70	2.70	16.70	205.70	43.70	2.70	43.70
16	Noise Spectral Density [dBm/Hz]	-186.37	-194.29	-186.37	-175.47	-182.20	-194.29	-182.20
17	Received P_t/N_0 [dB-Hz]	86.15	86.11	86.11	86.07	86.07	86.07	86.09
18	Data Rate, R [dB-Hz]	71.46	71.46	71.46	71.46	71.46	71.46	71.46
19	Available E_b/N_0 (17-18) [dB]	14.69	14.65	14.65	14.61	14.61	14.61	14.63
20	Required E_b/N_0 [dB]	11.60	11.60	11.60	11.60	11.60	11.60	11.60
21	**E_b/N_0 Margin (19-20) [dB]**	**3.09**	**3.05**	**3.05**	**3.01**	**3.01**	**3.01**	**3.03**

M≡Mars, P≡Phobos, S≡Satellite, E≡Earth, C≡Cycler, D.≡Downlink, U.≡Uplink.

Table 5.5 above proves that the maximum power inputs, and transmitter and receive antenna diameters specified in Table 5.4 can provide strong-enough communication links for continuous communication between the colonies on Phobos and Mars, and the Earth, as the E_b/N_0 margin for each communication link of the mission (row 21 in Table 5.5) is above the minimum required 3 dB E_b/N_0 margin.

6 Conclusions

The first part of this study (Sec. 2) describes the methodology followed to successfully prove the existance, in a circular-coplanar model, of a periodic propellant-free trajectory around the Sun that could enable a cost-efficient human transportation system from Earth to Mars in a future human exploration (and colonization) mission to Mars: the so-called ballistic Earth-Mars S1L1 cycler trajectory. The parameters that completely define the trajectory of the cycler vehicles (semi-major axis, eccentricity and argument of periapsis) are provided, as well as the relative velocities with respect to Earth and Mars, and the time-of-flight between the subsequent encounters with the planets. A ballistic cycler trajectory, however, was lately determined not to be possible in the ephemeris-model study performed by the Mission Design Team of Project Aldrin-Purdue.

The second part of this study (Sec. 3) proves, in a circular-coplanar model and in an ephemeris model, the capability of the cycler vehicles (if two cycler vehicles are used for human transportation to Mars–only one cycler vehicle would not be sufficient) to provide an alternative communication link between Earth and Mars during Earth-Mars solar conjunction. The use of the cycler vehicles as communication relays could enable uninterrupted communication between Earth and the colonies on Mars and Phobos in a future mission to Mars; in this way, the cycler vehicles are not used only for human transportation to Mars, but they are also used as communication satellites, which avoids the need of an additional heliocentric communications satellite constellation.

In a circular-coplanar model, two solutions for the communications satellite constellation around Mars are proposed and compared in the third part of the study (Sec. 4), which could enable a continuous communication link between the colonies on Phobos and Mars, and the Earth (direct communication to Earth or relayed by the cycler vehicles), with only two communication satellites in orbit around Mars (instead of the well-known three- or four-satellite constellation). Two satellites in a stationary orbit around Mars are determined to be a more convenient and efficient solution than two satellites in Phobos' orbit in terms of power requirements, number of antennas, quality of the communication links (based on the atmospheric attenuation) and maximum latitude of the colony on Mars for which the solutions are valid. The solutions here provided, however, do not provide complete coverage of the Martian surface.

Finally, in the fourth part of the study (Sec. 5) the link budget analysis for the communication architecture consisting of two areostationary satellites, the cycler vehicles, the colonies on Phobos and Mars, and the Earth is performed. Antenna diameters, power requirements and frequency of the signal are specified for the communication architecture to be able to transmit an HDTV communication signal from the colonies on Phobos and Mars to Earth.

The study here performed, then, describes a complete solution to continuously communicate with human colonies on Mars and Phobos in a future colonization mission to Mars, while minimizing the initial mass in low-Earth orbit of the mission.

7 References

[1] Rall, C. S., *Free-Fall Periodic Orbits Connecting Earth and Mars*, Sc.D. Dissertation, Department of Aeronautics and Astronautics, Massachusetts Institute of Technology, Cambridge, Massachusetts, October, 1969.

[2] Rall, C. S., and Hollister, W. M., *Free-Fall Periodic Orbits Connecting Earth and Mars*, AIAA Paper No. 71-92, January, 1971.

[3] Aldrin, E. E., *Cyclic Trajectory Concepts*, Science Applications International Corporation, Aerospace Systems Group, Hermosa Beach, California, October, 1985.

[4] Niehoff, J., *Manned Mars Mission Design*, Steps to Mars, Joint AIAA/Planetary Society Conference, National Academy of Sciences, July, 1985.

[5] Niehoff, J., *Integrated Mars Unmanned Surface Exploration (IMUSE), A New Strategy for the Intensive Science Exploration of Mars*, National Academy of Science Space Science Board Major Directions Summer Study, July, 1985.

[6] Niehoff, J., *Pathways to Mars: New Trajectory Opportunities*, American Astronautical Society, AAS Paper No. 86-172, July, 1986.

[7] Friedlander, A. L., Niehoff, J. C., Byrnes, D. V., and Longuski, J. M., *Circulating Transportation Orbits between Earth and Mars*, AIAA Paper No. 86-2009, August, 1986.

[8] Byrnes, D. V., Longuski, J. M., and Aldrin, B., *Cycler Orbit Between Earth and Mars*, Journal of Spacecraft and Rockets, Vol. 30, No. 3, pp. 334336, 1993.

[9] Byrnes, D. V., McConaghy, T. T., and Longuski, J. M., *Analysis of Various Two Synodic Period Earth-Mars Cycler Trajectories*, AIAA Paper No. 2002-4423, August, 2002.

[10] Chen, K. J., McConaghy, T. T., Okutsu, M., and Longuski, J. M., *A Low-Thrust Version of the Aldrin Cycler*, AIAA Paper No. 2002-4421, August, 2002.

[11] Chen, K. J., Landau, D. F., McConaghy, T. T., Okutsu, M., Longuski, J. M., and Aldrin, B., *Preliminary Analysis and Design of Powered Earth-Mars Cycling Trajectories*, AIAA Paper No. 2002-4422, August, 2002.

[12] Chen, K. J., McConaghy, T. T., Landau, D. F., Longuski, J. M., and Aldrin, B., *Powered EarthMars Cycler with Three-Synodic-Period Repeat Time*, Journal of Spacecraft and Rockets, Vol. 42, No. 5, pp. 921927, 2005.

[13] McConaghy, T. T., Yam, C. H., Landau, D. F., and Longuski, J. M., *Two-Synodic Period EarthMars Cyclers with Intermediate Earth Encounter*, American Astronautical Society, AAS Paper No. 03-509, August, 2003.

[14] McConaghy, T. T., Longuski, J. M., and Byrnes, D. V., *Analysis of a Class of EarthMars Cycler Trajectories*, Journal of Spacecraft and Rockets, Vol. 41, No. 4, pp. 622628, 2004.

[15] McConaghy, T. T., Longuski, J. M., and Byrnes, D. V., *Analysis of a Broad Class of Earth-Mars Cycler Trajectories*, AIAA Paper No. 2002-4420, August, 2002.

[16] McConaghy, T.T., Landau, D.F., Yam, C.H., and Longuski, J.M., *Notable Two-Synodic-Period Earth-Mars Cycler*, Journal of Spacecraft and Rockets, Vol. 43, No. 2, pp. 456-465, March-April 2006.

[17] Stevenson, S.M., *An Evolutionary Communication Scenario for Mars Exploration*, The CASE Mars III: Strategies for Exploration-Technical, Extract AAS No. 87-268, Vol. 75, 1990.

[18] Pernicka, H., et al., *Use of Halo Orbits to Provide a Communication Link between Earth and Mars*, AIAA Paper No. 92-4585-CP, AIAA/ASS Astrodynamics Conference, 1992.

[19] Palamarik, T., et al., *Mission Design for an Aerosynchronous Orbiter*, AAS Paper No. 89-197, AIAA/ASS Astrodynamics Conference, 1989.

[20] Draim, J.E., *A Common-Period Four-Satellite Continuous Global Coverage Constellation*, Journal of Guidance, Control and Dynamics, Vol. 10, No. 5, pp. 492-499, September-October, 1987.

[21] Draim, J.E., *Continuous Global N-Tuple Coverage with (2N+2) Satellites*, Jounal of Guidance, Control and Dynamics, Vol. 14, No. 1, pp. 1, January-February, 1991.

[22] Danehy, M., *Martian Communication Network Design Trade Study*, Master's Thesis, San José State University, December, 1997.

[23] Hopkins, R., *Long-Term Revisit Coverage Using Multi-Satellite Constellations*, AIAA Paper No. 88-4276, AIAA/ASS Astrodynamics Conference, Minneapolis, Minnesota, August, 1988.

[24] Hamilton, C., *Phobos 1 and 2 to Mars*, NASA National Space Science Data Center, Washington, D.C., 1994.

[25] Tai, W.K.F., *Mars Communication Network Design Trade Study*, Master's Thesis, San José State University, 1998.

[26] Mortari, D., Wilkins, M.P., and Bruccoleri, C., *The Flower Constellations*, The Journal of the Astronautical Sciences, Special Issue: The John L. Junkins Astrodynamics Symposium, Vol. 52, No. 1-2, pp. 107-127, January-June 2004.

[27] De Sanctis, M., Rossi, T., Lucente, M., Ruggieri, M., Mortari, D., and Izzo, D., *Flower Constellation of Orbiters for Martian Communication*, IEEEAC Paper No. 1324, 2007.

[28] McKay, R.J., Macdonald, M., Bosquillon de Frescheville, F., Vasile, M., McInnes, C.R., and Biggs, J.D., *Non-Keplerian Orbits using Low Thrust, High ISP Propulsion Systems*, 60th International Astronautical Congress, Daejeon, Korea, October, 2009.

[29] Bhasin, K., and Hayden, J.L., *Evolutionary Space Communications Architectures for Human/Robotic Exploration and Science Missions*, Nasa Technical Reports Server No. E-14550, April, 2004.

[30] Aldrin, B., David, L., *Mission to Mars: My Vision for Space Exploration*, National Geographic Society, May, 2013.

[31] Jordan, J.F., *The Application of Lambert's Theorem to the Solution of Interplanetary Transfer Problems*, Technical Report No. 32-521, Jet Propulsion Laboratory, Pasadena, California, February, 1964.

[32] Morabito, D., and Hastrup, R., *Communications with Mars during Periods of Solar Conjunction: Initial Study Results*, IPN Progress report, pp. 42-147, Jet Propulsion Laboratory, Pasadena, California, November, 2001.

[33] Basilevsky, A.T., Lorenz, C.A., Shingareva, T.V., et al., *The Surface Geology and Geomorphology of Phobos*, Planetary and Space Science, 2014.

[34] Larson, W.J., and Wertz, J.R., eds., *Space Mission Analysis & Design*, Microcosm, Torrance, California, 1992.

[35] Taylor, J., Cheung, K.M., and Seo, D., *Galileo Telecommunications*, Jet Propulsion Laboratory, Pasadena, California, July, 2002.

[36] Taylor, J., Sakamoto, L., and Wong, C.J., *Cassini Orbiter/Huygens Probe Telecommunications*, Jet Propulsion Laboratory, Pasadena, California, January, 2002.

[37] Taylor, J., *Dawn Telecommunications*, Jet Propulsion Laboratory, Pasadena, California, August, 2009.

[38] Mukai, R., Hansen, D., Mittskus, A., Taylor, J., and Danos, M., *Juno Telecommunications*, Jet Propulsion Laboratory, Pasadena, California, October, 2012.

[39] Makovsky, A., Barbieri, A., and Tung, R., *Juno Telecommunications*, Jet Propulsion Laboratory, Pasadena, California, July, 2002.

[40] Taylor, J., Makovsky, A., Barbieri, A., Tung, R., Estabrook, P. and Thomas, A.G., *Mars Exploration Rover Telecommunications*, Jet Propulsion Laboratory, Pasadena, California, October, 2005.

[41] Ho, C., Kantak, A., Slobin, S., and Morabito, D., *Link Analysis of a Telecommunication System on Earth, in: Geostationary Orbit, and at the Moon: Atmospheric Attenuation and Noise Temperature Effects*, Interplanetary Network Progress Report, pp. 42-168, October-December 2006, Jet Propulsion Laboratory, Pasadena, California, February, 2007.

[42] Ho, C., Slobin, S., Sue, M., and Njoku, E., *Mars Background Noise Temperatures Received by Spacecraft Antennas*, IPN Progress Report, pp. 42-149, Jet Propulsion Laboratory, Pasadena, California, May, 2002.

[43] Kouadio, A., *HDTV Services: Trends and Implementations*, ABU Digital Broadcasting Symposium 2009, European Broadcasting Union, Kuala Lumpur, Malaysia, 2009.

[44] Cominetti, M., Morello, A., and Visintin, M., *Wide RF-Band Digital HDTV Emission Systems: Performance of Advanced Channel Coding and Modulation Techniques*, European Broadcasting Union Technical Review Spring 1992, European Broadcasting Union, Geneva, 1992.

[45] Cominetti, M., et al., *HDTV Receiver Requirements*, European Broadcasting Union Tech 3333, European Broadcasting Union, Geneva, March, 2009.